

NATIONAL ADVISORY COMMITTEE FOR AERONAUTICS

TECHNICAL NOTE 2283

METHOD FOR CALCULATING LIFT DISTRIBUTIONS FOR UNSWEPT
WINGS WITH FLAPS OR AILERONS BY USE OF
NONLINEAR SECTION LIFT DATA

By James C. Sivells and Gertrude C. Westrick

SUMMARY

A method is presented which allows the use of nonlinear section lift data in the calculation of the spanwise lift distribution of unswept wings with flaps or ailerons. This method is based upon lifting-line theory and is an extension to the method described in NACA Rep. 865. The mathematical treatment of the discontinuity in absolute angle of attack at the end of the flap or aileron involves the use of a correction factor which accounts for the inability of a limited trigonometric series to represent adequately the spanwise lift distribution. A treatment of the apparent discontinuity in maximum section lift coefficient is also described. In order to minimize the computing time and to illustrate the procedures involved, simplified computing forms containing detailed examples are given for both symmetrical and asymmetrical lift distributions. A few comparisons of calculated characteristics with those obtained experimentally are also presented.

INTRODUCTION

Unswept-wing characteristics calculated by the method of reference 1, in which nonlinear section lift data are used, have been found to agree much closer with experimental data in the region of maximum lift coefficient than those calculated by methods in which linear section lift curves are used. It appears feasible that the similar use of nonlinear section data would yield improved results for unswept wings with flaps or ailerons. The deflection of a partial-span flap or aileron, however, causes discontinuities in the spanwise distribution of the absolute angle of attack. If such discontinuities exist, an excessively large number of spanwise stations must be considered in order to obtain a solution by the method of reference 1 or by any other method in which the lift distribution is approximated by a trigonometric series. A different method of treatment of the discontinuity is therefore desirable. Developed herein is a new method of treatment involving the use of a

correction factor which accounts for the inability of a limited trigonometric series to represent adequately the spanwise lift distribution of a wing with partial-span flaps or ailerons deflected. This correction factor is obtained with the aid of reference 2 and is used in conjunction with the system of multipliers of reference 1 to obtain the induced angle of attack from the spanwise lift distribution. The subsequent calculation of the lift distribution by means of successive approximations is similar to that of reference 1.

The mathematical treatment of the discontinuity in the spanwise distribution of absolute angle of attack is only part of the problem involved in calculations for wings with flaps or ailerons. The direct use of two-dimensional lift data would indicate a discontinuity in the spanwise distribution of maximum section lift coefficient. Obviously, the flow about the wing sections near the end of a flap or aileron is not two-dimensional. A rational method of obtaining three-dimensional section data from the two-dimensional data has therefore been devised and is presented herein. This method is substantiated by experimental pressure distributions.

In addition to the presentation of the method of making the calculations, simplified computing forms are given and their use is illustrated by detailed examples for both symmetrical and asymmetrical distributions. A few comparisons of calculated results with experimental data are also given.

This paper and reference 1 are intended to supplement each other. The reader is therefore expected to be reasonably familiar with reference 1.

SYMBOLS

As used herein, the term "section" designates the characteristic of a section in three-dimensional flow.

A	aspect ratio
A_n	coefficients of trigonometric series for lift distribution
C_{D_i}	induced drag coefficient
C_L	wing lift coefficient
C_l	rolling-moment coefficient
C_{n_i}	induced yawing-moment coefficient

E	edge-velocity factor for symmetrical part of lift distribution
E'	edge-velocity factor for antisymmetrical part of lift distribution
F	factor used in altering two-dimensional lift curves
R	Reynolds number
S	pressure coefficient $\left(\frac{\text{Total pressure} - \text{Local static pressure}}{\text{Dynamic pressure}} \right)$
a_0	section lift-curve slope per degree
b	span of wing
c	local chord of wing
c_s	root chord
\bar{c}	mean geometric chord (b/A)
c_{d_i}	section induced-drag coefficient
c_l	section lift coefficient
Δc_l	stall margin
$c_{l_{\max}}$	maximum section lift coefficient
$(c_{l_{\max}_0})$	maximum two-dimensional lift coefficient
$\Delta c_{l_{\max}}$	increment in maximum lift coefficient due to flap deflection (two-dimensional data)
c_l^*	section lift coefficient at either end of flap or aileron
c_{l_1}	section lift coefficient for part of lift distribution involving no discontinuity in angle of attack
c_{l_2}	section lift coefficient for part of lift distribution due to discontinuity in angle of attack
$c_{l_{al}}$	section lift coefficient for additional lift distribution
c_n	section normal-force coefficient

$\frac{pb}{2V}$	wing-tip helix angle generated by rolling wing
s, t	intervals used in integration
$\frac{t}{c}$	airfoil thickness-chord ratio
y	spanwise coordinate
y^*	spanwise coordinate at either end of flap or aileron
α	angle of attack, degrees
α_c	correction for induced angle of attack, degrees
α_e	effective angle of attack, degrees
$\Delta\alpha_e$	correction for effective angle of attack, degrees
α_i	induced angle of attack, degrees
α_{i1}	induced angle of attack for part of lift distribution involving no discontinuity in angle of attack, degrees
α_{i2}	induced angle of attack containing discontinuity, degrees
α_{i0}	angle of attack for zero lift, degrees
α_o	angle of attack for two-dimensional lift curves, degrees
α_s	angle of attack of root section, degrees
α_u	uncorrected induced angle of attack, degrees
β_{mk}	multiplier for induced angle of attack for asymmetrical distributions
γ_{mk}	multiplier for induced angle of attack for antisymmetrical distributions
δ	magnitude of discontinuity, in absolute and induced angles of attack, degrees
ϵ	angle of twist, negative if washout, degrees
ϵ_t	angle of twist at wing tip, degrees

$\bar{\epsilon}$	average angle of twist
ϵ_{δ}	faired angle of twist due to flap deflection
$\bar{\epsilon}_{\delta}$	average angle of twist due to flap deflection
η	ratio of actual two-dimensional lift-curve slope to theoretical value of $\pi^2/90$
η_m	area multiplier for asymmetrical distributions
η_{ms}	area multiplier for symmetrical distributions
$\theta = \cos^{-1} \frac{\partial y}{b}$	
$\theta^* = \cos^{-1} \frac{\partial y^*}{b}$	
λ	taper ratio $\left(\frac{\text{Tip chord}}{\text{Root chord}} \right)$
λ_{mk}	multiplier for induced angle of attack for symmetrical distributions
v_m	interpolation multiplier
σ_m	moment multiplier for asymmetrical distributions
σ_{ma}	moment multiplier for antisymmetrical distributions
*	used as superscript to denote value at end of flap or aileron

DEVELOPMENT OF METHOD

Lift Distribution

The method involving the use of multipliers to obtain the induced angle of attack from the spanwise lift distribution was presented in reference 1. In this development, the lift distribution was approximated by a finite trigonometric series

$$\left(\frac{c_l c}{b} \right)_m = \sum_{n=1}^{r-1} A_n \sin n \frac{m\pi}{r} \quad (1)$$

where $\cos \frac{m\pi}{r} = \frac{2y}{b}$ and $m = 1, 2, 3, \dots, r - 1$. From the values of $c_l c/b$ for each value of m , the induced angle of attack could then be obtained at the points $k\pi/r$ by the relation

$$\alpha_{i_k} = \sum_{m=1}^{r-1} \left(\frac{c_l c}{b} \right)_m \beta_{mk} \quad (2)$$

where $k = 1, 2, 3, \dots, r - 1$ and β_{mk} denotes the multipliers for asymmetrical distributions. The corresponding multipliers, λ_{mk} and γ_{mk} , are used for symmetrical and antisymmetrical distributions, respectively. These multipliers are tabulated in reference 1 for $r = 20$. The method can be used directly so long as there is no discontinuity in the spanwise distribution of absolute angle of attack caused by the deflection of a partial-span flap or aileron.

Lifting-line theory requires that a discontinuity in the distribution of absolute angle of attack must be accompanied by an identical discontinuity in the distribution of induced angle of attack in order to avoid a discontinuity in the spanwise lift distribution. An analytic expression for the lift distribution associated with a discontinuity in induced angle of attack is presented in reference 2. The complete lift distribution can thus be expressed as the sum of two distributions

$$\frac{c_l c}{b} = \frac{c_{l1} c}{b} + \delta \left(\frac{c_{l2} c}{b\delta} \right) \quad (3)$$

where $c_{l2} c/b\delta$ is the distribution due to a unit discontinuity in the induced angle of attack and $c_{l1} c/b$ is the remainder of the lift distribution. These distributions are illustrated in figure 1. Since no discontinuity is associated with the distribution $c_{l1} c/b$, the corresponding induced angle of attack can be obtained by means of the multipliers

$$\alpha_{i_{1k}} = \sum_{m=1}^{r-1} \left(\frac{c_{l1} c}{b} \right)_m \beta_{mk} \quad (4)$$

By definition, over the flap span

$$\alpha_{i_{2k}} = \delta \quad (5a)$$

and over the unflapped span

$$\alpha_{i2k} = 0 \quad (5b)$$

The total induced angle of attack is

$$\alpha_{ik} = \alpha_{i1k} + \alpha_{i2k} \quad (6)$$

If, however, the multipliers were used with the total distribution

$$\sum_{m=1}^{r-1} \left(\frac{c_{l1c}}{b} \right)_m \beta_{mk} = \sum_{m=1}^{r-1} \left(\frac{c_{l1c}}{b} \right)_m \beta_{mk} + \sum_{m=1}^{r-1} \delta \left(\frac{c_{l2c}}{b\delta} \right)_m \beta_{mk}$$

and α_{i2k} were added to both sides of this equation, the result would be

$$\begin{aligned} \sum_{m=1}^{r-1} \left(\frac{c_{l1c}}{b} \right)_m \beta_{mk} + \alpha_{i2k} &= \sum_{m=1}^{r-1} \left(\frac{c_{l1c}}{b} \right)_m \beta_{mk} + \alpha_{i2k} + \sum_{m=1}^{r-1} \delta \left(\frac{c_{l2c}}{b\delta} \right)_m \beta_{mk} \\ &= \alpha_{i1k} + \sum_{m=1}^{r-1} \delta \left(\frac{c_{l2c}}{b\delta} \right)_m \beta_{mk} \end{aligned}$$

Rearranging this expression gives

$$\alpha_{ik} = \sum_{m=1}^{r-1} \left(\frac{c_{l1c}}{b} \right)_m \beta_{mk} + \delta \left[\frac{\alpha_{i2k}}{\delta} - \sum_{m=1}^{r-1} \left(\frac{c_{l2c}}{b\delta} \right)_m \beta_{mk} \right] \quad (7)$$

A comparison of equation (7), for a wing with a flap or aileron, with equation (2), for a wing without flap or aileron, shows the addition of a term which is proportional to the magnitude of the discontinuity and acts as a correction factor to account for the inability of a limited trigonometric series to represent adequately the spanwise lift distribution of a wing with partial-span flaps or ailerons deflected. For simplicity, equation (7) may be written as

$$\alpha_{ik} = \alpha_{uik} + \delta \left(\frac{\alpha_{c_k}}{\delta} \right) \quad (8)$$

where the uncorrected induced angle of attack is expressed as

$$\alpha_{u_k} = \sum_{m=1}^{r-1} \left(\frac{c_{l_2c}}{b} \right)_m \beta_{mk} \quad (9)$$

and the correction factor per unit discontinuity is given by the equation

$$\frac{\alpha_{c_k}}{\delta} = \frac{\alpha_{i_2k}}{\delta} - \sum_{m=1}^{r-1} \left(\frac{c_{l_2c}}{b\delta} \right)_m \beta_{mk} \quad (10)$$

The distribution $c_{l_2c}/b\delta$ given in reference 2 may be expressed in the form

$$\frac{c_{l_2c}}{b\delta} = \frac{1}{90} \left[(\cos \theta - \cos \theta^*) \log_e \frac{1 - \cos(\theta + \theta^*)}{1 - \cos(\theta - \theta^*)} + \frac{\pi \theta^* \sin \theta}{90} \right] \quad (11)$$

for $\frac{\alpha_{i_2}}{\delta} = 1$, $0^\circ < \theta < \theta^*$; for $\frac{\alpha_{i_2}}{\delta} = 0$, $\theta^* < \theta < 180^\circ$; and θ^* and δ are in degrees. This distribution is dependent on only the spanwise position of the discontinuity and is independent of aspect ratio and taper ratio. The correction factor per unit discontinuity α_{c_k}/δ given by equation (10) is therefore a function of only the spanwise position of the discontinuity. The distribution of α_{i_2}/δ , for which equation (11) applies, is illustrated in figure 2(a). Values of $c_{l_2c}/b\delta$ corresponding to this type of distribution are presented in table I for various values of $2y/b$ and $2y^*/b$. These values are plotted against $2y/b$ in figure 3 for even increments in $2y^*/b$ and against $2y^*/b$ in figure 4 for even increments in $\theta = \cos^{-1} \frac{2y}{b}$. In table II are given values of α_c/δ corresponding to the values of $c_{l_2c}/b\delta$ of table I.

The distribution of α_{i_2}/δ illustrated in figure 2(a) would be applicable only for a wing with one outboard flap or aileron deflected. For a wing with symmetrical inboard flaps, the distribution would be obtained as illustrated in figure 2(b) and the values of α_c/δ would be obtained in like manner. For example, for a wing with flaps extending from $\frac{2y^*}{b} = 0.6$ to $\frac{2y^*}{b} = -0.6$, the values of α_c/δ to be used would be obtained by subtracting the values of α_c/δ for $\frac{2y^*}{b} = 0.6$

from those for $\frac{2y^*}{b} = -0.6$. Since the resulting distribution would be symmetrical, the values of α_c/δ would also be symmetrical. Similarly, an antisymmetrical distribution of α_{l2}/δ and the corresponding values of α_c/δ would be obtained as illustrated in figure 2(c).

It should be noted that two values of α_c/δ exist at the end of the flap, one corresponding to $\frac{2y^*}{b} + 0$ (flap side of $2y^*/b$) and one corresponding to $\frac{2y^*}{b} - 0$ (unflapped side). Only the values corresponding to $\frac{2y^*}{b} + 0$ are given in table II. For the unflapped side,

$$\left(\frac{\alpha_c}{\delta}\right)_{\frac{2y^*}{b}-0} = \left(\frac{\alpha_c}{\delta}\right)_{\frac{2y^*}{b}+0} - 1$$

These values have no practical significance unless the discontinuity occurs at one of the stations $\frac{2y}{b} = \cos \frac{k\pi}{r}$. At these stations, either of the two values may be used so long as the value is used with the proper section lift curve.

In the calculation of the induced angle of attack by equation (8), the values of α_{ck}/δ must be multiplied by the magnitude of the discontinuity δ . The value of δ to be used is obtained from the section lift curves at the lift coefficient c_l^* . If the discontinuity occurs at one of the spanwise stations $\frac{2y}{b} = \cos \frac{k\pi}{r}$, the value of $(c_{l2}c/b)^*$ is obtained as one of the values of $c_{l2}c/b$ computed. If the discontinuity occurs at some other position, the value of $(c_{l2}c/b)^*$ must be interpolated. This interpolation may be accomplished in the following manner. Even though the spanwise lift distribution is continuous through this point, the point is singular. Its singularity is due to the singularity of the corresponding point of the distribution of $c_{l2}c/b\delta$ which has an infinite slope but zero radius of curvature. At this point, from equation (11),

$$\left(\frac{c_{l2}c}{b\delta}\right)^* = \frac{\pi\theta^* \sin \theta^*}{8100} \quad (12)$$

Since both the distribution of $c_{l2}c/b$ and the distribution of $c_{l2}c/b\delta$ contain the same type of singularity, a curve with $c_{l2}c/b$ as the dependent variable and $c_{l2}c/b\delta$ as the independent variable would have no singular

point and could be approximated by a polynomial for which Lagrange's interpolation formula (reference 3) is applicable. From Lagrange's formula

$$\left(\frac{c_l c}{b}\right)^* = \sum_m \left(\frac{c_l c}{b}\right)_m v_m \quad (13)$$

where

$$v_m = \frac{\prod_{\substack{k=1 \\ k \neq m}}^{n+1} \left[\left(\frac{c_{l_2} c}{b\delta}\right)^* - \left(\frac{c_{l_2} c}{b\delta}\right)_k \right]}{\prod_{\substack{k=1 \\ k \neq m}}^{n+1} \left[\left(\frac{c_{l_2} c}{b\delta}\right)_m - \left(\frac{c_{l_2} c}{b\delta}\right)_k \right]} \quad (14)$$

The number $(n + 1)$ of terms retained determines the degree (n) of the polynomial used in the approximation. It has been found that using four terms (two on each side of the desired point), which define a third-degree curve, gives values at the end of the flap which agree within about 1 percent with the values obtained by means of the method of reference 4 but with about 45 terms of a trigonometric series. Values of the interpolation multipliers determined in this manner are presented in table III for various spanwise positions of the end of a flap. This type of interpolation is suitable only if the variables are single-valued in the range of the interpolation. This limitation precludes the determination of multipliers for $\frac{2y^*}{b} = 0.1$ but this position is out of the range of practical flap spans.

The method of determining the lift distribution by means of successive approximations is the same as that of reference 1 with the added step of determining the correction factor α_c . For a given geometric angle of attack, the lift distribution is assumed. The uncorrected induced angle of attack is determined by equation (9) for asymmetrical distributions or by a corresponding equation using λ_{mk} for symmetrical distributions. The multipliers γ_{mk} for antisymmetrical distributions can be used only if the lift curves are linear and the value of δ is independent of lift coefficient. The value of $(c_l c/b)^*$ is obtained by means of equation (13) and is divided by $(c/b)^*$ to determine c_l^* . At this value of c_l^* , δ is read from the section lift curves as the difference between the effective angle of attack for the section without the flap and that for the section with the flap, both at the station at

the end of the flap. This value of δ is multiplied by the appropriate values of α_c/δ from table II to obtain α_c . The values of α_c are added to the uncorrected values α_u to obtain the values of induced angle of attack which are then subtracted from the geometric angle of attack to give the effective angle of attack at each spanwise station. At each value of effective angle of attack, the corresponding value of c_l is read from the appropriate section lift curve and multiplied by the value of c/b at that station to obtain a check value of $c_l c/b$. If the check values do not agree with those originally assumed, a second approximation is made and the process is repeated. Further approximations are made until one is found which is in agreement with the check values.

Determination of Three-Dimensional Section Data

If the two-dimensional lift data were used directly, a discontinuity in the spanwise distribution of maximum lift coefficient would be indicated at the end of the deflected flap or aileron. Inasmuch as this discontinuity does not exist in three-dimensional flow, some means of altering the two-dimensional data must be used to obtain what may be called three-dimensional section data. One method of alteration is described in reference 5 for use with linear section lift data. In order to use this method, the lift distribution must be broken up into the basic lift distribution due to twist and the additional lift distribution due to angle of attack. When nonlinear section lift data are used, the lift distribution cannot be broken up in this manner and the method of reference 5 is not applicable. For this reason, the method hereinafter described has been developed. Although this development is not rigorous, the reasoning behind it is substantiated by experimental pressure distributions.

The foundation of the method used herein is the calculation of two curves for which linear section lift data are used. One curve, the spanwise distribution of section lift coefficient for a wing with flaps but no other twist, is calculated by the method described herein but adapted for linear lift curves in a manner similar to that of reference 1. The other curve is the additional lift-coefficient distribution (constant absolute angle-of-attack distribution) calculated as in reference 1. These curves may be calculated for any convenient angle of attack and for any convenient value for the discontinuity in angle of attack at the end of the flap. A typical set of curves is shown in figure 5. It is reasoned that the root section of a wing with partial-span flaps would be acting most nearly like that of a wing with full-span flaps so that the additional lift-coefficient distribution is multiplied by a suitable constant to give the same value at the root. Likewise, it is reasoned that the tip section would be acting most nearly like that of a wing without flaps so that the additional

lift-coefficient distribution is multiplied by another constant to give the same value at the outermost station used in the computations (the 0.9877-semispan station when 10 points on the semispan are used). The differences between the values on the curves are then divided by the difference between the values on the additional lift-coefficient curves at the end of the flap to obtain the factor F shown in figure 6 for several wings. In order to interpolate for the points on the additional lift-coefficient curves at the end of the flap, the multipliers μ_m , presented in table IV, have been determined. These multipliers were obtained by using θ as the independent variable in equation (14) instead of $c_{l2}c/b\delta$. It can be readily seen that the factor F is independent of the angle of attack and magnitude of the discontinuity used in the original computations. The factor F is also relatively independent of lift-curve slope so that it can be used near maximum lift where the lift curves are nonlinear.

The maximum lift-coefficient values are altered by means of the factor F according to the relation

$$c_{l_{\max}} = (c_{l_{\max}})_c + F(\Delta c_{l_{\max}}^*) \quad (15)$$

The values of c_l and α are then altered according to the equations

$$\frac{(c_l)_{\text{altered}}}{(c_l)_{\text{unaltered}}} = \frac{c_{l_{\max}}}{(c_{l_{\max}})_o} \quad (16)$$

$$\frac{\alpha_e - \alpha_{l0}}{\alpha_o - \alpha_{l0}} = E \frac{c_{l_{\max}}}{(c_{l_{\max}})_o} \quad (17)$$

The edge-velocity factor E is used in the same manner as in reference 1. The value of E given in reference 6 is, however, probably more accurate than the ratio of semiperimeter to span used in reference 1. From reference 6 for unswept wings,

$$E = \sqrt{1 + \frac{4}{A^2}} \quad (18)$$

The foregoing description of the alteration to the two-dimensional section data has been limited to wings with symmetrical partial-span flaps. For wings with deflected ailerons, a similar method based upon the same reasoning could readily be devised.

The reasoning behind the method of altering the two-dimensional data is substantiated by the results shown in figures 7 and 8 and obtained from experimental pressure distributions for a wing of aspect ratio of 6.0, taper ratio of 0.5, and NACA 64-210 airfoil sections. Chordwise pressure distributions were obtained at six spanwise stations. Two spans of flaps, 0.49b and 0.51b, were tested so that the pressure distribution at $\frac{2y}{b} = 0.5$ was obtained, in one case, just outboard of the end of the flap and, in the other case, just inboard of the end of the flap. As shown in figure 7, the pressure distributions at each station are very similar for the two flap spans, even at the station 0.5b/2. Furthermore, there is a gradual spanwise change from the type of loading associated with an airfoil section with flaps to the type associated with a plain airfoil.

For comparative purposes, the section normal-force coefficients, obtained by integration of the chordwise pressure distributions at each spanwise station, together with calculated values of section lift coefficient, interpolated for the same spanwise station, are shown in figure 8. The calculations for the flaps-neutral and full-span-flaps configuration were made according to reference 1 and those for the partial-span-flaps configuration were made as described herein. For the experimental data, jet-boundary and stream-angle corrections have been applied to the angle of attack, but no corrections have been applied to the values of c_n for the effects of the model supports and the boom containing the pressure tubes. Although some of the disagreement shown may be attributed to the assumptions involved in the calculations, most of it is believed to be due to experimental inaccuracies both in the two-dimensional data used in the calculations and in the three-dimensional data shown herein, inasmuch as similar disagreement is evident for the full-span configuration as for the partial-span configuration. In general, however, the trends indicated in figure 8 serve to substantiate the method used to alter two-dimensional data.

Wing Characteristics

Numerical integration.- In the numerical integration described in reference 1, the multipliers η_m , η_{ms} , σ_m , and σ_{ma} were determined by harmonic analysis. For example, it was shown that

$$\int_{-1}^1 f\left(\frac{2y}{b}\right) d\left(\frac{2y}{b}\right) = 2 \sum_{m=1}^{r-1} f\left(\frac{2y}{b}\right)_m \frac{\pi}{2r} \sin \frac{m\pi}{r} \quad (19)$$

where $\frac{\pi}{2r} \sin \frac{m\pi}{r}$ was designated as η_m . By inspection, it may be seen

that equation (19) could also be obtained through the application of the trapezoidal rule (reference 3) where $f(2y/b)_m \sin(m\pi/r)$ is the function of $m\pi/r$ and the interval between points is π/r . Although equation (19) may be expected to give good results when $f(2y/b)$ is approximately elliptic, in general the application of Simpson's (parabolic) rule to this problem has been found to give better results for a wider variety of curve shapes. Since r was originally assumed to be even, the interval $m = 0$ to r may be divided into $r/2$ regions, the area of each of which is

$$\frac{\pi}{3r} \left[f\left(\frac{2y}{b}\right)_i \sin \frac{i\pi}{r} + 4f\left(\frac{2y}{b}\right)_{i+1} \sin \frac{(i+1)\pi}{r} + f\left(\frac{2y}{b}\right)_{i+2} \sin \frac{(i+2)\pi}{r} \right] \quad (20)$$

For the entire interval $m = 0$ to r ,

$$\begin{aligned} \int_{-1}^1 f\left(\frac{2y}{b}\right) d\left(\frac{2y}{b}\right) &= 2 \sum_{m=1}^{r-1} f\left(\frac{2y}{b}\right)_m \frac{\pi}{6r} \left[3 - (-1)^m \right] \sin \frac{m\pi}{r} \\ &= 2 \sum_{m=1}^{r-1} f\left(\frac{2y}{b}\right)_m \eta_m \end{aligned} \quad (21)$$

where η_m is defined and used herein as

$$\eta_m = \frac{\pi}{6r} \left[3 - (-1)^m \right] \sin \frac{m\pi}{r} \quad (22)$$

The relations between η_m , η_{ms} , σ_m , and σ_{ms} are the same as in reference 1; namely,

$$\eta_{ms} = 2\eta_m \quad \left(m \neq \frac{r}{2}\right) \quad (23a)$$

$$\eta_{ms} = \eta_m \quad \left(m = \frac{r}{2}\right) \quad (23b)$$

$$\sigma_m = \frac{\eta_m}{2} \cos \frac{m\pi}{r} \quad (24)$$

$$\begin{aligned}\sigma_{ma} &= 2\sigma_m \\ &= \eta_m \cos \frac{m\pi}{r}\end{aligned}\quad (25)$$

Values of η_m , η_{ms} , σ_m , and σ_{ma} are given in table V for $r = 20$.

For cases for which the end of the flap or aileron is at a point where m is not an even integer, a special form of equation (20) is required which gives additional multipliers for numerical integration in the vicinity of the end of the flap or aileron. Such a case is illustrated in figure 9 and the individual areas are

$$\text{Area (1)} = \frac{\pi}{r} \left[\frac{s(2s + 3t)}{6(s + t)} f_1 + \frac{s(s + 3t)}{6t} f_2 - \frac{s^3}{6(s + t)t} f_3 \right] \quad (26)$$

$$\text{Area (2)} = \frac{\pi}{r} \left[-\frac{t^3}{6s(s + t)} f_1 + \frac{t(t + 3s)}{6s} f_2 + \frac{t(2t + 3s)}{6(s + t)} f_3 \right] \quad (27)$$

$$\text{Area (1) + (2)} = \frac{\pi}{r} \left[\frac{(2s - t)(s + t)}{6s} f_1 + \frac{(s + t)^3}{6st} f_2 + \frac{(2t - s)(s + t)}{6t} f_3 \right] \quad (28)$$

where s and t are expressed as fractions of π/r . It can be seen that equation (28) is the same as expression (20) when $s = t = 1$. An example of the computation of these special multipliers is given in table VI for 0.5-span flaps. For the area B in the sketch accompanying this table, equation (28) is used with $s = 1$ and $t = \frac{1}{3}$, and for the area C, equation (26) is used with $s = \frac{2}{3}$ and $t = 1$. Values of the η_{ms} multipliers are given in table VII for various locations of the end of a flap. Values of the multipliers η_m , σ_m , and σ_{ma} can be readily obtained from the values of η_{ms} by means of equations (23) to (25).

It should be noted that two multipliers are given at the end of the flap. For distributions which are continuous through the end of the flap, such as the distribution of $c_l c/b$, the sum of the two multipliers may be used. For distributions which are discontinuous at this point, such as the distribution of $c_{d1} c/b$, each multiplier should be used separately with its appropriate value. For example, for $\frac{2y^*}{b} = 0.5$, the

multiplier -0.03023 should be used with the value at the outboard end of the flap, and the multiplier 0.03930 should be used with the value at the inboard end of the unflapped span.

Wing coefficients.- The formulas derived in reference 1 are repeated herein for convenience. For asymmetrical distributions

$$C_L = A \sum_{m=1}^{r-1} \left(\frac{c_l c}{b} \right)_m \eta_m \quad (29a)$$

For symmetrical distributions

$$C_L = A \sum_{m=1}^{r/2} \left(\frac{c_l c}{b} \right)_m \eta_{ms} \quad (29b)$$

For asymmetrical distributions

$$C_{D_i} = \frac{\pi A}{180} \sum_{m=1}^{r-1} \left(\frac{c_l c}{b} \alpha_i \right)_m \eta_m \quad (30a)$$

For symmetrical distributions

$$C_{D_i} = \frac{\pi A}{180} \sum_{m=1}^{r/2} \left(\frac{c_l c}{b} \alpha_i \right)_m \eta_{ms} \quad (30b)$$

For asymmetrical distributions

$$C_l = -A \sum_{m=1}^{r-1} \left(\frac{c_l c}{b} \right)_m \sigma_m \quad (31a)$$

For antisymmetrical distributions

$$C_l = -A \sum_{m=1}^{\frac{r-1}{2}} \left(\frac{c_l c}{b} \right)_m \sigma_{ma} \quad (31b)$$

For asymmetrical distributions

$$C_{n_i} = \frac{\pi A}{180} \sum_{m=1}^{r-1} \left(\frac{c_l c}{b} \alpha_i \right)_m \sigma_m \quad (32)$$

The values of η_m , η_{ms} , σ_m , and σ_{ma} should be used as defined herein, and the summations should also include the special multipliers in the vicinity of the end of the flap or aileron.

ILLUSTRATIVE EXAMPLES

Symmetrical Distributions

The method described is applied herein to a wing, the geometric characteristics of which are given in table VIII. The section lift curves are shown in figure 10 as dotted lines before being altered and as solid lines after being altered. The unaltered data are obtained by interpolation of two-dimensional data for the proper Reynolds number and airfoil thickness-chord ratio for each spanwise station in a manner similar to that of reference 1. The altered curves are obtained as described previously and are used in the calculation of the lift distributions in tables IX and X. These tables were designed for use with calculating machines capable of performing accumulative multiplication. The mechanics of computing are explained in the tables, but a few items need additional explanation.

The initial approximation of $c_l c/b$ is obtained in table IX. The computations in this table are based on the method of reference 6, the pertinent equations of which are modified to suit the present purpose. The spanwise stations, at which values of $c_l c/b$ are computed, are listed in column (1). Columns (2) to (4) are used to obtain the additional lift distribution $c_{l_{al}} c/\bar{c}$ for $C_L = 1$ according to the approximate relation

$$\frac{c_{l_{al}} c}{\bar{c}} \approx \frac{1}{2} \left[\frac{c}{\bar{c}} + \frac{4}{\pi} \sqrt{1 - \left(\frac{2y}{b} \right)^2} \right] \quad (33)$$

Columns (5) to (7) are used to obtain faired values of the twist ϵ_δ due to flap deflection according to the relations

$$\epsilon_\delta = \frac{\delta}{2} \left[1 + \sqrt{1 - \left(\frac{2y}{2y^*} \right)^2} \right] \quad \left(0 < \frac{2y}{b} < \frac{2y^*}{b} \right) \quad (34a)$$

$$\epsilon_{\delta} = \frac{\delta}{2} \left[1 - \sqrt{1 - \left(\frac{1 - \frac{2y}{b}}{1 - \frac{2y^*}{b}} \right)^2} \right] \quad \left(\frac{2y^*}{b} < \frac{2y}{b} < 1 \right) \quad (34b)$$

This fairing is illustrated in figure 11. Columns (8) and (9) are used to obtain the average twist $\bar{\epsilon}_{\delta}$ according to the equation

$$\bar{\epsilon}_{\delta} = \sum_{m=1}^{r/2} \left(\frac{c_{l_{al}c}}{\bar{c}} \right)_m \epsilon_{\delta_m} \eta_{ms} \quad (35)$$

The value of $\bar{\epsilon}_{\delta}$ obtained by this summation is given at the bottom of the table. Columns (10) to (12) are used to obtain an angle of attack α' defined, for the flapped span, as

$$\alpha' = \frac{AE + 2}{AE + 6} (\epsilon_{\delta} - \bar{\epsilon}_{\delta}) + \bar{\epsilon}_{\delta} - \delta + \alpha \quad (36a)$$

and, for the unflapped span, as

$$\alpha' = \frac{AE + 2}{AE + 6} (\epsilon_{\delta} - \bar{\epsilon}_{\delta}) + \bar{\epsilon}_{\delta} + \alpha \quad (36b)$$

The values of the geometric angle of attack α in column (11) include the values of continuous twist ϵ . Values of $c_l(\alpha')$ in column (13) are obtained for the section lift curves at the angle α' . In the non-linear range of the section lift curves, different values of $c_l^*(\alpha')$ are found corresponding to the two values of α' at the end of the flaps. For the purpose of this table, the average value of $c_l^*(\alpha')$ is used. Finally, columns (14) and (15) are used to obtain the initial approximate values of $c_l c/b$ according to the relation

$$\left(\frac{c_l c}{b} \right)_{\text{approx}} = \frac{c_{l_{al}c}}{\bar{c}(AE + 2)} c_l(\alpha') \quad (37)$$

which was adapted from the equation

$$\frac{c_l c}{b} \approx \frac{\alpha_{\infty}}{AE + 2} \frac{c_{l_{al}c}}{\bar{c}} \left[\bar{\epsilon} + \frac{AE + 2}{AE + 6} (\epsilon - \bar{\epsilon}) \right] \quad (38)$$

given in reference 6.

The value of δ used in table IX should correspond to the value of c_l^* obtained at the bottom of the table. Some value of δ must be selected, however, for the computations needed to determine the value of c_l^* . It is therefore advisable to omit the computations in columns (10) to (15), except the bottom row, until a value of δ has been found by trial and error which is consistent with the value of c_l^* .

If the lift distribution is to be obtained at a relatively high angle of attack, as in the example shown, the values of α' may be in the rapidly curving part of the section lift curves or even greater than the angle of attack for maximum section lift coefficient. For the purpose of this table, the section lift curves may be extended in the general direction of the nearly linear part of the curves in order to obtain the values of $c_l(\alpha')$. This procedure is justified inasmuch as the subsequent operation in column (15) will reduce the value of c_l .

The approximate values of $c_l c/b$ (column (15), table IX) are used in column (3) of table X and the computations indicated are performed. Except for the computation of α_c , the computations in this table are the same as those in reference 1 for wings without flaps. The value of δ used in column (16) is obtained at the section lift coefficient c_l^* corresponding to the value of $(c_l c/b)^*$ obtained by means of the interpolation multipliers v_m .

In this method of successive approximations, the value of $c_l c/b$ in column (22) will usually not check the initial approximate values in column (3). The values to be used in subsequent approximations may be found by the equation

$$\Delta' \left(\frac{c_l c}{b} \right)_m = \frac{1}{K} \sum_{i=0}^{r-1} K_i \Delta \left(\frac{c_l c}{b} \right)_{m+i} \quad (39)$$

where $\Delta'(c_l c/b)$ is the increment to be added to the approximate values to obtain succeeding approximate values, $\Delta(c_l c/b)$ is the difference between the check values and the approximate values (column (22) minus column (3)), and K and K_i are constants for any particular wing. Equation (39) is derived in the appendix, and values of K and K_i for $r = 20$ are presented in figure 12 as functions of AE/η . These values compare favorably with those empirically determined in reference 1 ($K_0 = 3$, $K_1 = 1$, $K_{i>1} = 0$, and $K = 8$ to 10). Although these values were obtained for elliptic wings, they can be used for wings of other plan form. The number of terms of equation (39) needed for any particular approximation depends upon the convergence of the approximation; fewer terms are needed when the differences $\Delta(c_l c/b)$ are small or when positive differences nearly cancel negative differences. Values of K_i for values of i greater than 3 are small enough to be considered negligible.

Some additional explanation of the use of equation (39) may be desirable. For values of m from 3 to 7, equation (39) may be used directly if the constants $K_{1>3}$ are neglected. For values of m from 8 to 10, equation (39) may be expanded as

$$\Delta' \left(\frac{c_l c}{b} \right)_8 = \frac{1}{K} \left[K_3 \Delta \left(\frac{c_l c}{b} \right)_5 + K_2 \Delta \left(\frac{c_l c}{b} \right)_6 + K_1 \Delta \left(\frac{c_l c}{b} \right)_7 + \right. \\ \left. K_0 \Delta \left(\frac{c_l c}{b} \right)_8 + (K_1 + K_3) \Delta \left(\frac{c_l c}{b} \right)_9 + K_2 \Delta \left(\frac{c_l c}{b} \right)_{10} \right] \quad (40a)$$

$$\Delta' \left(\frac{c_l c}{b} \right)_9 = \frac{1}{K} \left[K_3 \Delta \left(\frac{c_l c}{b} \right)_6 + K_2 \Delta \left(\frac{c_l c}{b} \right)_7 + (K_1 + K_3) \Delta \left(\frac{c_l c}{b} \right)_8 + \right. \\ \left. (K_0 + K_2) \Delta \left(\frac{c_l c}{b} \right)_9 + K_1 \Delta \left(\frac{c_l c}{b} \right)_{10} \right] \quad (40b)$$

$$\Delta' \left(\frac{c_l c}{b} \right)_{10} = \frac{1}{K} \left[2K_3 \Delta \left(\frac{c_l c}{b} \right)_7 + 2K_2 \Delta \left(\frac{c_l c}{b} \right)_8 + 2K_1 \Delta \left(\frac{c_l c}{b} \right)_9 + K_0 \Delta \left(\frac{c_l c}{b} \right)_{10} \right] \quad (40c)$$

for symmetrical distributions, since $\Delta \left(\frac{c_l c}{b} \right)_j = \Delta \left(\frac{c_l c}{b} \right)_{r-j}$. For values of m of 1 and 2, equation (39) may be expanded as

$$\Delta' \left(\frac{c_l c}{b} \right)_1 = \frac{1}{K} \left[(K_0 - K_2) \Delta \left(\frac{c_l c}{b} \right)_1 + (K_1 - K_3) \Delta \left(\frac{c_l c}{b} \right)_2 + \right. \\ \left. K_2 \Delta \left(\frac{c_l c}{b} \right)_3 + K_3 \Delta \left(\frac{c_l c}{b} \right)_4 \right] \quad (41a)$$

$$\Delta' \left(\frac{c_l c}{b} \right)_2 = \frac{1}{K} \left[(K_1 - K_3) \Delta \left(\frac{c_l c}{b} \right)_1 + K_0 \Delta \left(\frac{c_l c}{b} \right)_2 + K_1 \Delta \left(\frac{c_l c}{b} \right)_3 + \right. \\ \left. K_2 \Delta \left(\frac{c_l c}{b} \right)_4 + K_3 \Delta \left(\frac{c_l c}{b} \right)_5 \right] \quad (41b)$$

since

$$\Delta\left(\frac{c_l c}{b}\right)_{-j} = -\Delta\left(\frac{c_l c}{b}\right)_j$$

After convergence is obtained in table X, the values of $c_l c/b$ (column (3)) and α_1 (column (18)) are entered in table XI and the lift and induced-drag coefficients are determined through use of the appropriate multipliers η_{ms} .

Asymmetrical Distributions

If the angle-of-attack distribution is not symmetrical, the asymmetrical multipliers β_{mk} must be used in the nonlinear range of the section lift curves. Typical asymmetrical distributions are those for a rolling wing or for a wing with deflected ailerons. Illustrated in table XII is the case of a wing with flaps but without deflected ailerons, which is rolling at such a rate that the tip helix angle $pb/2V$ generated is 0.01 radian or 0.573° . Added to the normal angle of attack is an increment equal to $\frac{2y}{b} \frac{pb}{2V}$ (in deg), which is the equivalent twist of the rolling wing. In order to reduce the size of the computing form, the table of the multipliers β_{mk} is arranged in the form shown. The values of β_{mk} for a positive value of $2y/b$ are the reverse of those for the corresponding negative value. Instead of reversing the values of β_{mk} in table XII, the values of $c_l c/b$ are written in reverse order in column (14). Using these values with the values of β_{mk} gives the uncorrected angle α_u for the stations listed at the bottom of the table.

In general, the value of δ will be different for the two sides of the wing, so that the appropriate values must be used with columns (16) and (17). The values of α_c/δ_- in column (16) are those for $\frac{2y^*}{b} = -0.6$ from table II, while the values of α_c/δ_+ in column (17) are the negative of those for $\frac{2y^*}{b} = 0.6$.

Another modification must be made for asymmetrical lift distributions since the edge-velocity factor E' should be used for the antisymmetrical part of the distribution (see reference 6), whereas the edge-velocity factor E has been used to alter the two-dimensional lift curves. From reference 6 for unswept wings,

$$E' = \sqrt{1 + \frac{16}{A^2}} \quad (42)$$

This value may be taken into account in the following manner: The symmetrical part of the effective angle distribution is

$$\frac{(\alpha - \alpha_1)_k + (\alpha - \alpha_1)_{r-k}}{2}$$

which is used directly with the altered lift curves. The antisymmetrical increment in the angle distribution is

$$(\alpha - \alpha_1)_k - (\alpha - \alpha_1)_{r-k}$$

which must be multiplied by the ratio E/E' in order for it to be used with the same lift curve. The effective angle is therefore

$$\begin{aligned} \alpha_e &= \frac{(\alpha - \alpha_1)_k + (\alpha - \alpha_1)_{r-k}}{2} + \frac{E}{E'} \frac{(\alpha - \alpha_1)_k - (\alpha - \alpha_1)_{r-k}}{2} \\ &= (\alpha - \alpha_1)_k - \frac{E' - E}{2E'} \left[(\alpha - \alpha_1)_k - (\alpha - \alpha_1)_{r-k} \right] \\ &= \alpha - \alpha_1 - \Delta\alpha_e \end{aligned} \quad (43)$$

where

$$\Delta\alpha_e = \frac{E' - E}{2E'} \left[(\alpha - \alpha_1)_k - (\alpha - \alpha_1)_{r-k} \right] \quad (44)$$

Equation (44) is computed in column (21) of table XII.

Other than these modifications, the computing required for table XII is similar to that for table X.

DISCUSSION

The lift characteristics of two wings without flaps and with 60-percent and full-span flaps have been calculated by the method described herein and are presented in figure 13 together with experimental results from reference 7. One wing had NACA 64-210 sections and was equipped with split flaps. The other wing had NACA 65-210 sections and was equipped with split, single slotted, and double slotted flaps. For the split-flap conditions, the agreement between calculated and experimental results is quite satisfactory, whereas the agreement is less

satisfactory for the single- and double-slotted-flap conditions. Since the discrepancies occur for both the 60-percent-span and full-span conditions, they are probably due to differences between the two-dimensional and three-dimensional section characteristics rather than due to the method of calculating. Some of the discrepancies in maximum lift coefficient may be due to the fact that the characteristics of these wings were extremely sensitive to small surface irregularities.

The stalling characteristics of these same wing-flap combinations are presented in figure 14 together with the calculated stall-margin distributions. The stall margin Δc_l is the difference between the maximum section lift coefficient altered as described herein and the section lift coefficient at the maximum wing lift coefficient. The spanwise location of zero margin should correspond to the location of initial stall, and the margin at other spanwise locations is an indication of the manner in which the stall spreads. In general, the agreement between the experimental and calculated stalling characteristics is very good.

The foregoing comparisons between calculated and experimental results were made for the same Reynolds number. If possible, such comparisons should be made at the same Mach number also, unless the Mach number is low enough to have a negligible effect. Even at relatively low values of free-stream Mach number, adverse compressibility effects on maximum lift coefficient have been noted (reference 8) when sonic velocity is reached locally on a wing. Similar effects in two-dimensional flow have not as yet been thoroughly investigated so that calculations based on available two-dimensional data must be limited to subcritical Mach numbers.

Langley Aeronautical Laboratory
National Advisory Committee for Aeronautics
Langley Field, Va., November 13, 1950

APPENDIX

DETERMINATION OF COEFFICIENTS USED TO
OBTAIN SUCCEEDING APPROXIMATIONS

In the method of successive approximations to determine the lift distribution, it is desirable to reach convergence with a minimum number of approximations. This desideration necessitates that each successive approximation be obtained from preceding computations in some manner. The manner in which these operations were performed in reference 1 and the coefficients used therein were determined empirically. It is shown hereinafter, however, that the procedure and similar coefficients can be determined theoretically.

In the following derivation, $\Delta(c_l c/b)$ is used to designate the difference between the check values and the approximate values, and $\Delta'(c_l c/b)$ is used to designate the increment to be added to the approximate values to obtain the succeeding approximate values. The section lift curves are assumed to be linear and δ to be zero. The operations performed during the first approximation (table X) may then be represented by the equation

$$\left\{ \alpha_k - \sum_m \lambda_{mk} \left(\frac{c_l c}{b} \right)_m \right\} \left(\frac{a_0 c}{b} \right)_k = \left(\frac{c_l c}{b} \right)_k + \Delta \left(\frac{c_l c}{b} \right)_k \quad (A1)$$

If suitable increments $\Delta'(c_l c/b)$ are chosen so that the check values become equal to the approximate values for the second approximation,

$$\left\{ \alpha_k - \sum_m \lambda_{mk} \left(\frac{c_l c}{b} + \Delta' \frac{c_l c}{b} \right)_m \right\} \left(\frac{a_0 c}{b} \right)_k = \left(\frac{c_l c}{b} \right)_k + \Delta' \left(\frac{c_l c}{b} \right)_k \quad (A2)$$

The difference between these equations is

$$\left(\frac{a_0 c}{b} \right)_k \sum_m \lambda_{mk} \Delta' \left(\frac{c_l c}{b} \right)_m = \Delta \left(\frac{c_l c}{b} \right)_k - \Delta' \left(\frac{c_l c}{b} \right)_k \quad (A3)$$

From reference 1

$$\lambda_{kk} = \frac{180r}{8\pi \sin \frac{k\pi}{r}} \quad (A4)$$

The lift-curve slope may be expressed as

$$a_o = \frac{\eta}{E} \frac{\pi^2}{90} \quad (A5)$$

where η is the ratio of the actual two-dimensional lift-curve slope to the theoretical thin-airfoil value. For elliptic wings,

$$\left(\frac{c}{b}\right)_k = \frac{4}{\pi A} \sin \frac{k\pi}{r} \quad (A6)$$

Therefore

$$\left(\frac{a_o c}{b}\right)_k \lambda_{kk} = \frac{\eta r}{AE} \quad (A7)$$

which, for constant η , is constant for all spanwise stations. Substituting this value into equation (A3) yields

$$\left(1 + \frac{AE}{\eta r}\right) \Delta' \left(\frac{c_l c}{b}\right)_k + \sum_{m \neq k} \frac{\lambda_{mk}}{\lambda_{kk}} \Delta' \left(\frac{c_l c}{b}\right)_m = \frac{AE}{\eta r} \Delta \left(\frac{c_l c}{b}\right)_k \quad (A8)$$

Equation (A8) represents $r/2$ simultaneous equations which may be represented in matrix form as

$$\left[M \right] \left[\Delta' \frac{c_l c}{b} \right] = \frac{AE}{\eta r} \left[\Delta \frac{c_l c}{b} \right] \quad (A9)$$

where $[M]$ is a matrix with all the principal diagonal elements equal to $1 + \frac{AE}{\eta r}$ and the other elements are $\lambda_{mk}/\lambda_{kk}$. This matrix can readily be put into a symmetrical form and its reciprocal obtained by one of the standard methods presented in reference 9. Then

$$\left[\Delta' \frac{c_l c}{b} \right] = \frac{AE}{\eta r} [M]^{-1} \left[\Delta \frac{c_l c}{b} \right] \quad (A10)$$

For a given value of AE/η , equation (A10) may be expressed in the form

$$\Delta' \left(\frac{c_l c}{b}\right)_m = \frac{1}{K} \sum_{i=0}^{r-1} K_i \Delta \left(\frac{c_l c}{b}\right)_{m+i} \quad (A11)$$

because of the particular properties of this reciprocal matrix. For convenience K_1 is made equal to unity and the values of K and K_1 are adjusted accordingly. The values given in table XIII and figure 12 were obtained for various values of AE/η and $r = 20$.

REFERENCES

1. Sivells, James C.; and Neely, Robert H.: Method for Calculating Wing Characteristics by Lifting-Line Theory Using Nonlinear Section Lift Data. NACA Rep. 865, 1947.
2. Multhopp, H.: Die Berechnung der Auftriebsverteilung von Tragflügeln. Luftfahrtforschung, Bd. 15, Lfg. 4, April 6, 1938, pp. 153-169. (Available as R.T.P. Translation No. 2392, British M.A.P.).
3. Sokolnikoff, Ivan S., and Sokolnikoff, Elizabeth S.: Higher Mathematics for Engineers and Physicists. Second ed., McGraw-Hill Book Co., Inc., 1941, pp. 552-559.
4. Taylor, J. Lockwood: The Lift Distribution on a Twisted Elliptic Wing, with Special Reference to the Effect of Flaps. Jour. R.A.S., vol. XXXIX, no. 300, Dec. 1935, pp. 1154-1156.
5. Pearson, Henry A., and Anderson, Raymond F.: Calculation of the Aerodynamic Characteristics of Tapered Wings with Partial-Span Flaps. NACA Rep. 665, 1939.
6. Sivells, James C.: An Improved Approximate Method for Calculating Lift Distributions Due to Twist. NACA TN 2282, 1951.
7. Sivells, James C., and Spooner, Stanley H.: Investigation in the Langley 19-Foot Pressure Tunnel of Two Wings of NACA 65-210 and 64-210 Airfoil Sections with Various Type Flaps. NACA Rep. 942, 1949.
8. Furlong, G. Chester, and Fitzpatrick, James E.: Effects of Mach Number up to 0.34 and Reynolds Number up to 8×10^6 on the Maximum Lift Coefficient of a Wing of NACA 66-Series Airfoil Sections. NACA TN 2251, 1950.
9. Frazer, R. A., Duncan, W. J., and Collar, A. R.: Elementary Matrices and Some Applications to Dynamics and Differential Equations. The Macmillan Co., 1946.

TABLE I.- LIFT DISTRIBUTION, $\frac{c_{l2}^c}{b^2} \times 10^2$, AT STATIONS $\frac{2x}{b}$ DUE TO DISCONTINUITY IN INDUCED ANGLE OF ATTACK AT STATIONS $\frac{2x}{b}$

$\frac{2x}{b}$	-0.9877	-0.9511	-0.8910	-0.8090	-0.7071	-0.5878	-0.4540	-0.3090	-0.1564	0	0.1564	0.3090	0.4540	0.5878	0.7071	0.8090	0.8910	0.9511	0.9877	$y = y^*$	$y = -y^*$
-1.0000	1.0921	2.1573	3.1695	4.1035	4.9365	5.6430	6.2804	6.8594	7.3820	7.8480	8.2584	8.6136	8.9144	9.1608	9.3536	9.4944	9.5832	9.6192	9.6016	9.5296	9.4032
-0.9877	1.0375	2.1382	3.1572	4.0946	4.9296	5.6423	6.2157	6.7384	7.2012	7.6032	7.9444	8.2248	8.4544	8.6328	8.7600	8.8368	8.8624	8.8376	8.7632	8.6384	8.4640
-0.9511	0.8941	1.9416	3.0640	4.0295	4.8796	5.6023	6.1826	6.6572	7.0248	7.3872	7.7448	8.0976	8.4552	8.8176	9.1848	9.5568	9.9336	10.3152	10.7016	11.0928	11.4880
-0.9000	0.7960	1.6550	2.7901	3.8700	4.7627	5.5102	6.1074	6.5451	6.9133	7.2112	7.5384	7.8948	8.2800	8.6944	9.1376	9.6096	10.1008	10.6112	11.1416	11.6912	12.2592
-0.8510	0.7820	1.6223	2.6940	3.8334	4.7370	5.4902	6.0812	6.5117	6.8796	7.1848	7.5272	7.9072	8.3248	8.7784	9.2584	9.7648	10.2976	10.8568	11.4416	12.0528	12.6896
-0.8090	0.6773	1.3686	2.1901	3.2828	4.4279	5.2600	5.8839	6.3611	6.7818	7.1344	7.5184	7.9344	8.3816	8.8592	9.3672	9.9048	10.4712	11.0664	11.6896	12.3408	13.0192
-0.8000	0.6677	1.3686	2.1901	3.2828	4.4279	5.2600	5.8839	6.3611	6.7818	7.1344	7.5184	7.9344	8.3816	8.8592	9.3672	9.9048	10.4712	11.0664	11.6896	12.3408	13.0192
-0.7071	0.5732	1.1812	1.8361	2.5990	3.4756	4.3833	5.2996	6.1257	6.8674	7.5312	8.1168	8.6240	9.0528	9.5024	9.9728	10.4640	10.9752	11.5064	12.0576	12.6288	13.2192
-0.7000	0.5732	1.1812	1.8361	2.5990	3.4756	4.3833	5.2996	6.1257	6.8674	7.5312	8.1168	8.6240	9.0528	9.5024	9.9728	10.4640	10.9752	11.5064	12.0576	12.6288	13.2192
-0.6000	0.4963	1.0087	1.5573	2.1723	2.8533	3.5024	4.1184	4.6912	5.2208	5.7120	6.1648	6.5784	6.9528	7.2872	7.5816	7.8352	8.0480	8.2192	8.3488	8.4272	8.4544
-0.5878	0.4877	0.9911	1.5292	2.1308	2.7833	3.4032	4.0000	4.5632	5.0912	5.5808	6.0312	6.4432	6.8160	7.1488	7.4416	7.6944	7.9072	8.0784	8.2072	8.2848	8.3112
-0.5000	0.4308	0.8738	1.3437	1.8610	2.4604	3.0248	3.5536	4.0448	4.4976	4.9120	5.2872	5.6224	5.9168	6.1696	6.3808	6.5504	6.6784	6.7544	6.7872	6.7776	6.7248
-0.4540	0.4036	0.8180	1.2562	1.7356	2.2845	2.8416	3.3072	3.7808	4.2624	4.7520	5.2496	5.7544	6.2656	6.7824	7.3048	7.8320	8.3640	8.9008	9.4424	9.9888	10.5400
-0.4000	0.3736	0.7567	1.1602	1.5996	2.0968	2.6049	3.0358	3.4896	3.9648	4.4512	4.9488	5.4576	5.9768	6.5056	7.0440	7.5920	8.1496	8.7168	9.2936	9.8800	10.4760
-0.3090	0.3272	0.6622	1.0136	1.3927	1.8160	2.2711	2.7472	3.2344	3.7320	4.2400	4.7584	5.2872	5.8264	6.3752	6.9336	7.5016	8.0792	8.6664	9.2632	9.8700	10.4864
-0.3000	0.3272	0.6622	1.0136	1.3927	1.8160	2.2711	2.7472	3.2344	3.7320	4.2400	4.7584	5.2872	5.8264	6.3752	6.9336	7.5016	8.0792	8.6664	9.2632	9.8700	10.4864
-0.2000	0.3229	0.6534	0.9999	1.3736	1.7902	2.2365	2.6989	3.1768	3.6696	4.1776	4.6992	5.2344	5.7824	6.3424	6.9144	7.4976	8.0912	8.6952	9.3088	9.9320	10.5648
-0.1564	0.2993	0.5839	0.8801	1.1747	1.5246	1.9251	2.4092	2.9056	3.4144	3.9344	4.4656	5.0072	5.5592	6.1216	6.6944	7.2776	7.8712	8.4752	9.0896	9.7144	10.3496
-0.1000	0.2367	0.4782	0.7298	0.9978	1.2909	1.6217	2.0115	2.4608	2.9704	3.5408	4.1712	4.8520	5.5832	6.3648	7.1968	8.0792	9.0112	10.0032	11.0560	12.1696	13.3440
0	0.1999	0.4035	0.6151	0.8395	1.0833	1.3576	1.6708	2.0244	2.4288	2.8832	3.3872	3.9408	4.5440	5.1968	5.9088	6.6800	7.5104	8.3992	9.3464	10.3520	11.4160
0.1000	0.1665	0.3360	0.5117	0.6975	0.8981	1.1203	1.3741	1.6759	2.0244	2.4288	2.8832	3.3872	3.9408	4.5440	5.1968	5.9088	6.6800	7.5104	8.3992	9.3464	10.3520
0.1564	0.1491	0.3009	0.4580	0.6238	0.8024	0.9984	1.2033	1.4280	1.6728	1.9376	2.2124	2.4972	2.7912	3.0944	3.4064	3.7272	4.0568	4.3952	4.7424	5.0976	5.4712
0.2000	0.1364	0.2751	0.4186	0.5699	0.7325	0.9144	1.1135	1.3300	1.5648	1.8176	2.0872	2.3728	2.6736	2.9888	3.3184	3.6624	4.0200	4.3912	4.7760	5.1744	5.5864
0.3000	0.1093	0.2203	0.3350	0.4595	0.5846	0.7298	0.8840	1.0567	1.2456	1.4504	1.6712	1.9080	2.1600	2.4272	2.7088	3.0048	3.3152	3.6400	3.9784	4.3304	4.6960
0.3090	0.1070	0.2156	0.3279	0.4458	0.5671	0.7101	0.8647	1.0330	1.2256	1.4312	1.6488	1.8776	2.1168	2.3664	2.6272	2.9000	3.1848	3.4816	3.7904	4.1120	4.4464
0.4000	0.0950	0.1712	0.2602	0.3535	0.4531	0.5615	0.6821	0.8199	0.9826	1.1835	1.4492	1.7046	2.0000	2.3248	2.6784	3.0512	3.4432	3.8544	4.2848	4.7336	5.2000
0.4540	0.0730	0.1471	0.2234	0.3034	0.3886	0.4812	0.5838	0.7044	0.8372	1.0040	1.2199	1.4894	1.8120	2.1672	2.5440	2.9424	3.3632	3.8064	4.2712	4.7576	5.2648
0.5000	0.0634	0.1277	0.1940	0.2634	0.3372	0.4172	0.5096	0.6098	0.7226	0.8638	1.0438	1.2712	1.5464	1.8688	2.2288	2.6160	3.0208	3.4432	3.8832	4.3400	4.8128
0.5878	0.0467	0.0941	0.1428	0.1937	0.2478	0.3052	0.3705	0.4428	0.5264	0.6260	0.7504	0.8936	1.0568	1.2392	1.4408	1.6632	1.9064	2.1704	2.4544	2.7584	3.0824
0.6000	0.0445	0.0897	0.1362	0.1848	0.2363	0.2919	0.3531	0.4219	0.5013	0.5958	0.7131	0.8676	1.0534	1.2608	1.4896	1.7392	2.0096	2.3008	2.6128	2.9456	3.2992
0.7000	0.0284	0.0572	0.0869	0.1178	0.1505	0.1877	0.2242	0.2713	0.3265	0.3844	0.4448	0.5072	0.5712	0.6368	0.7040	0.7732	0.8444	0.9168	0.9904	1.0656	1.1424
0.7071	0.0274	0.0552	0.0837	0.1135	0.1450	0.1788	0.2160	0.2574	0.3048	0.3504	0.4080	0.4672	0.5272	0.5888	0.6512	0.7152	0.7808	0.8480	0.9168	0.9872	1.0592
0.8090	0.0152	0.0306	0.0465	0.0630	0.0804	0.0991	0.1195	0.1421	0.1678	0.1977	0.2336	0.2736	0.3168	0.3632	0.4120	0.4624	0.5144	0.5680	0.6232	0.6800	0.7384
0.8000	0.0142	0.0285	0.0433	0.0587	0.0749	0.0932	0.1133	0.1363	0.1623	0.1912	0.2236	0.2592	0.2972	0.3376	0.3804	0.4256	0.4732	0.5224	0.5732	0.6256	0.6796
0.8910	0.0060	0.0121	0.0184	0.0249	0.0318	0.0392	0.0472	0.0560	0.0656	0.0760	0.0872	0.0992	0.1120	0.1256	0.1400	0.1552	0.1712	0.1880	0.2056	0.2240	0.2432
0.9000	0.0053	0.0107	0.0162	0.0219	0.0279	0.0344	0.0414	0.0492	0.0572	0.0656	0.0744	0.0836	0.0932	0.1032	0.1136	0.1244	0.1356	0.1472	0.1592	0.1716	0.1844
0.9111	0.0018	0.0036	0.0055	0.0074	0.0095	0.0117	0.0140	0.0166	0.0196	0.0230	0.0268	0.0312	0.0360	0.0412	0.0468	0.0528	0.0592	0.0660	0.0732	0.0808	0.0888
0.9877	0.0018	0.0036	0.0055	0.0074	0.0095	0.0117	0.0140	0.0166	0.0196	0.0230	0.0268	0.0312	0.0360	0.0412	0.0468	0.0528	0.0592	0.0660	0.0732	0.0808	0.0888

NACA

TABLE III.- INTERPOLATION MULTIPLIERS v_M FOR OBTAINING VALUES
OF $\left(\frac{c_l c^*}{b}\right)$ AT THE END OF THE FLAP

$\frac{2y}{b}$	0.2000	0.3000	0.4000	0.5000	0.6000	0.7000	0.8000	0.9000
0	-0.2970	-0.1839	0	0	0	0	0	0
.1564	1.0008	.3203	-.1940	0	0	0	0	0
.3090	.4269	.8957	.6203	-.1274	0	0	0	0
.4540	-.1307	-.0321	.6945	.7663	-.0477	-.0337	0	0
.5878	0	0	-.1208	.4786	.9112	.1234	-.0367	0
.7071	0	0	0	-.1175	.1876	.9433	.1534	0
.8090	0	0	0	0	-.0511	-.0330	.9277	-.0431
.8910	0	0	0	0	0	0	-.0444	.8901
.9511	0	0	0	0	0	0	0	.1951
.9877	0	0	0	0	0	0	0	-.0421



TABLE IV.- INTERPOLATION MULTIPLIERS μ_m FOR OBTAINING VALUES
 OF $\frac{c_{l_{al}}^c}{b}$ AT THE SPANWISE STATIONS $\frac{2y^*}{b}$

$\frac{2y^*}{b}$ \ / $\frac{2y}{b}$	0.2000	0.3000	0.4000	0.5000	0.6000	0.7000	0.8000	0.9000
0	-.0580	-.0100	0	0	0	0	0	0
.1564	.7908	.0620	-.0542	0	0	0	0	0
.3090	.3104	.9663	.4250	-.0617	0	0	0	0
.4540	-.0432	-.0183	.6928	.7407	-.0277	-.0106	0	0
.5878	0	0	-.0636	.3704	.9428	.0656	-.0160	0
.7071	0	0	0	-.0494	.1009	.9642	.1009	0
.8090	0	0	0	0	-.0160	-.0192	.9428	-.0350
.8910	0	0	0	0	0	0	-.0277	.9202
.9511	0	0	0	0	0	0	0	.1359
.9877	0	0	0	0	0	0	0	-.0211



TABLE V.- WING-COEFFICIENT MULTIPLIERS

$\frac{2y}{b}$	m	η_m	η_{ms}	σ_m	σ_{ma}
-0.9877	19	0.01638	-----	-0.00809	-----
- .9511	18	.01618	-----	- .00769	-----
- .8910	17	.04754	-----	- .02118	-----
- .8090	16	.03078	-----	- .01245	-----
- .7071	15	.07405	-----	- .02618	-----
- .5878	14	.04236	-----	- .01245	-----
- .4540	13	.09331	-----	- .02118	-----
- .3090	12	.04980	-----	- .00769	-----
- .1564	11	.10343	-----	- .00809	-----
0	10	.05236	0.05236	0	0
.1564	9	.10343	.20686	.00809	.01618
.3090	8	.04980	.09960	.00769	.01539
.4540	7	.09331	.18661	.02118	.04236
.5878	6	.04236	.08472	.01245	.02490
.7071	5	.07405	.14810	.02618	.05236
.8090	4	.03078	.06155	.01245	.02490
.8910	3	.04754	.09508	.02118	.04236
.9511	2	.01618	.03236	.00769	.01539
.9877	1	.01638	.03276	.00809	.01618

TABLE VI.- CALCULATION OF AREA MULTIPLIERS WITH SPECIAL CONSIDERATION AT THE END OF A 0.5-SPAN FLAP

$\frac{2y}{b}$	m	Factors for areas indicated							$\frac{\pi}{20} \sin \frac{\pi m}{20}$	η_{ms}
		A	B	C	D	E	F	Total		
0	10	$\frac{1}{3}$						$\frac{1}{3}$	0.157080	0.05236
.156	9	$\frac{4}{3}$						$\frac{4}{3}$.155146	.20686
.309	8	$\frac{1}{3}$	$\frac{10}{27}$					$\frac{19}{27}$.149392	.10513
.454	7		$\frac{32}{27}$					$\frac{32}{27}$.139959	.16588
.500	$6\frac{2}{3}$		$\frac{2}{9}$	$\frac{13}{45}$				$\frac{1}{15}$.136035	.00907
.588	6			$\frac{11}{27}$	$\frac{1}{3}$			$\frac{20}{27}$.127080	.09413
.707	5			$\frac{4}{135}$	$\frac{4}{3}$			$\frac{176}{135}$.111072	.14481
.809	4				$\frac{1}{3}$	$\frac{1}{3}$		$\frac{2}{3}$.092329	.06155
.891	3					$\frac{4}{3}$		$\frac{4}{3}$.071313	.09508
.951	2					$\frac{1}{3}$	$\frac{1}{3}$	$\frac{2}{3}$.048540	.03236
.988	1						$\frac{4}{3}$	$\frac{4}{3}$.024573	.03276

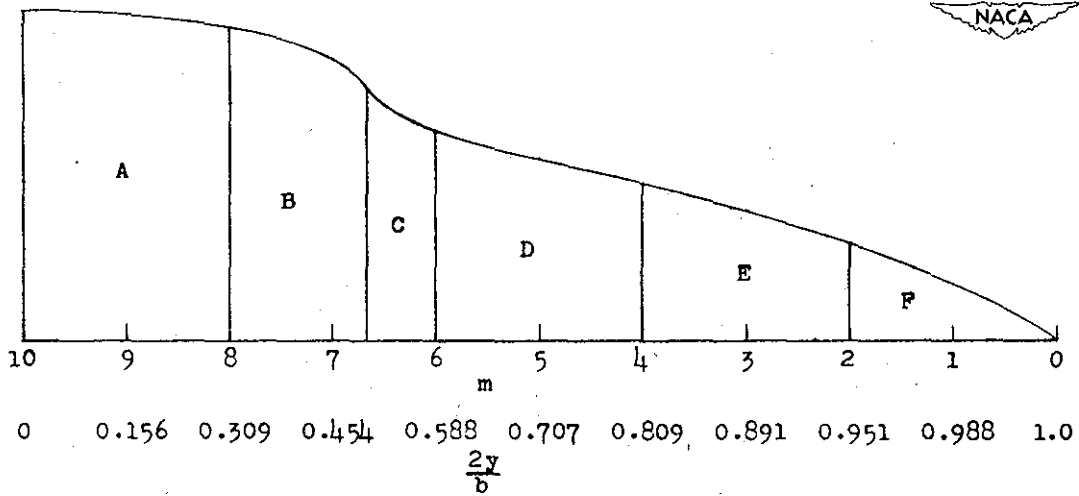


TABLE VII.- AREA MULTIPLIERS η_{ms} FOR VARIOUS SPANWISE LOCATIONS $\frac{2y^*}{b}$ OF THE END OF A FLAP

$\frac{2y^*}{b}$	0	0.1564	0.3090	0.4540	0.5878	0.7071	0.8090	0.8910	0.9511	0.9877	$\frac{2y^*}{b} - 0$	$\frac{2y^*}{b} + 0$
0.1000	0.06678	0.18044	0.10535	0.18661	0.08472	0.14810	0.06155	0.09508	0.03236	0.03276	0.03322	-0.02697
.1564	.10472	—	.14939	.17495	.08472	.14810	.06155	.09508	.03236	.03276	.05172	.06464
.2000	.05766	.19323	.11628	.18158	.08472	.14810	.06155	.09508	.03236	.03276	-.05089	.04756
.3000	.05384	.20082	.05439	.18661	.08472	.14810	.06155	.09508	.03236	.03276	.04534	.00443
.3090	.05236	.20686	—	.18661	.08472	.14810	.06155	.09508	.03236	.03276	.04980	.04980
.4000	.05236	.20306	.10566	.16131	.08971	.14810	.06155	.09508	.03236	.03276	.03892	-.02087
.4540	.05236	.19393	.14939	—	.12708	.13884	.06155	.09508	.03236	.03276	.05832	.05832
.5000	.05236	.20686	.10513	.16588	.09413	.14481	.06155	.09508	.03236	.03276	-.03023	.03930
.5878	.05236	.20686	.09960	.18661	—	.14810	.06155	.09508	.03236	.03276	.04236	.04236
.6000	.05236	.20686	.09960	.18659	.04870	.14130	.06290	.09508	.03236	.03276	.00589	.03560
.7000	.05236	.20686	.09960	.17672	.12042	.34991	.06247	.09508	.03236	.03276	.04405	-.27258
.7071	.05236	.20686	.09960	.17495	.12708	—	.09233	.08914	.03236	.03276	.04628	.04628
.8000	.05236	.20686	.09960	.18661	.08657	.14130	.03538	.09507	.03236	.03276	.02670	.00442
.8090	.05236	.20686	.09960	.18661	.08472	.14810	—	.09508	.03236	.03276	.03078	.03078
.8910	.05236	.20686	.09960	.18661	.08472	.13884	.09233	—	.04854	.03072	.02971	.02971
.9000	.05236	.20686	.09960	.18661	.08472	.14810	.06328	.13281	.04347	.03132	-.07434	.02520
.9511	.05236	.20686	.09960	.18661	.08472	.14810	.06155	.09508	—	.03276	.01618	.01618
.9877	.05236	.20686	.09960	.18661	.08472	.14810	.06155	.08914	.04854	—	.01024	.01231

NACA

TABLE VIII.- GEOMETRIC CHARACTERISTICS OF EXAMPLE WING

Taper ratio, λ	0.400	Root section	NACA 64-210
Aspect ratio, A	$\frac{9.021}{15.000}$	Tip section	NACA 64-210
Span, b, ft	15.000	Geometric twist, ϵ_t , deg	-2.00
Root chord, c_s , ft	$\frac{2.381}{4.44 \times 10^6}$	Edge-velocity factor, E	1.024
Wing Reynolds number, R	4.44×10^6	Edge-velocity factor, E'	1.094

$\frac{2y}{b}$	$\frac{c}{c_s}$	$\frac{c}{b}$	R	$\frac{t}{c}$	$\frac{\epsilon}{\epsilon_t}$	ϵ	v_m	$\frac{\alpha_c}{\delta}$	F	$(c_{l_{max}})_0$	$\frac{c_{l_{max}}}{(c_{l_{max}})_0}$
0	1.0000	0.1587	5.98×10^6	0.10	0	0	0	0.0006	0	2.027	1.0000
.1564	.9062	.1438	5.42	.10	.0690	-.14	0	.0015	-.0061	2.032	.9981
.3090	.8146	.1293	4.87	.10	.1517	-.30	0	.0031	-.0293	2.037	.9910
.4540	.7276	.1155	4.35	.10	.2496	-.50	-.0477	-.0068	-.0940	2.039	.9710
.5878	.6473	.1027	3.87	.10	.3632	-.73	.9112	.3154	-.3665	2.040	.8870
.7071	.5757	.0914	3.44	.10	.4913	-.98	.1876	.0878	.1779	1.401	1.0799
.8090	.5146	.0817	3.08	.10	.6288	-1.26	-.0511	-.0117	.0789	1.393	1.0356
.8910	.4654	.0739	2.78	.10	.7658	-1.53	0	.0122	.0304	1.383	1.0138
.9511	.4293	.0681	2.57	.10	.8862	-1.77	0	-.0036	.0085	1.376	1.0039
.9877	.3720	.0590	2.22	.10	.9698	-1.94	0	.0065	0	1.361	1.0000
$\frac{2y^*}{b} = 0.6$.6400	.1016	3.83	.10	.3750	-.75				2.040	.8626
										1.411	1.2471

For tapered wings with straight-line elements from root to construction tip.

$$\frac{c}{c_s} = 1 - (1 - \lambda) \frac{2y}{b}$$

(Alter values of c/c_s near tip to allow for rounding.)

$$\frac{\epsilon}{\epsilon_t} = \lambda \frac{2y/b}{c/c_s}$$

(Use value of c/c_s before rounding tip.)



TABLE IX.- CALCULATION OF INITIAL APPROXIMATION OF LIFT DISTRIBUTION FOR EXAMPLE WING WITH 0.6 SPAN FLAPS

$$A = \frac{9.021}{1.024}; E = \frac{1.024}{AE + 2} = 11.24; \frac{AE + 2}{AE + 6} = 0.7875; \alpha_S = \frac{10.00}{12.00}; \delta = \frac{12.00}{12.00}$$

(1)	(2)	(3)	(4)	(5)	(6)	(7)	(8)	(9)	(10)	(11)	(12)	(13)	(14)	(15)
$\frac{2y}{b}$	$\frac{c}{\bar{c}}$ $(A \times \frac{c}{b})$	$1.2732 \times \sqrt{1 - (1)^2}$	$\frac{c_1 c}{a_1 \bar{c}}$ $\frac{(2) + (3)}{2}$	$\frac{(1)}{2y^*}$ $\frac{1}{b}$ (a)	$\sqrt{1 - (5)^2}$	$\frac{\epsilon_0}{1 + (6)^2} \times \delta$ (a)	$(4) \times (7)$	η_{ms} (table VII)	$(\epsilon_0 - \bar{\epsilon}_0) \times \frac{AE + 2}{AE + 6}$	α $(\alpha_S + \epsilon)$	$\frac{\alpha'}{(10) + \bar{\epsilon}_0} + \frac{\bar{\epsilon}_0}{(11) - \delta}$ (a)	$c_i(\alpha')$ (Sect. data)	$\frac{(4)}{AE + 2}$	$\frac{c_i c}{b}$ (Approx.) $(13) \times (14)$
0	1.4320	1.2732	1.3526	0	1.0000	12.00	15.23	0.05236	2.83	10.00	8.93	2.164	0.1204	0.261
.1564	1.2977	1.2576	1.2777	.2607	.9654	11.79	15.06	.20886	2.68	9.86	8.70	2.160	.1137	.246
.3090	1.1665	1.2110	1.1888	.5150	.8572	11.14	13.24	.09860	2.20	9.70	8.03	2.096	.1058	.222
.4540	1.0419	1.1345	1.0882	.7567	.6538	9.92	10.79	.18659	1.30	9.50	6.96	2.014	.0968	.195
.5878	.9269	1.0300	.9785	.9797	.2005	7.20	7.05	.04870	-.71	9.27	4.72	1.772	.0871	.154
.7071	.8244	.9003	.8624	.7323	.6810	1.91	1.65	.14130	-4.61	9.02	12.57	1.394	.0767	.107
.8090	.7369	.7484	.7427	.4775	.8786	.73	.54	.06290	-5.48	8.74	11.42	1.285	.0661	.085
.8910	.6665	.5780	.6223	.2725	.9621	.23	.14	.09506	-5.85	8.47	10.78	1.230	.0554	.068
.9511	.6148	.3934	.5041	.1223	.9925	.05	.03	.03236	-5.98	8.23	10.41	1.197	.0449	.054
.9877	.5327	.1991	.3659	.0808	.9995	0	0	.03276	-6.02	8.06	10.20	1.176	.0326	.038
$\frac{2y^*}{b}$ 0.6	.9165	1.0186	.9676	1.0000	0	6.00	5.81	.04149	-1.59	9.25	3.82 15.82	1.693	.0861	.146
			$\frac{1 - (1)}{1 - 2y^*}$ $\frac{1}{b}$			$\frac{1 - (6)}{2} \times \delta$	$\bar{\epsilon}_0 = \sum (8) \times (9) = 8.16$				$\frac{(10) + \bar{\epsilon}_0}{(11)}$		$\frac{(c_i c)^*}{(AE + 2)} A$ $c_i^* = \frac{(c_i c)^*}{(\bar{c})} = 1.44$	

^a Operations indicated in column headings for $0 < \frac{2y}{b} < \frac{2y^*}{b}$; operations at bottom for $\frac{2y^*}{b} < \frac{2y}{b} < 1$.



TABLE X -- CALCULATION OF LIFT DISTRIBUTION FOR EXAMPLE WING WITH 0.5 SPAN FLAPS

(1)	(2)	(3)	(4)				(5)				(6)	(7)	(8)	(9)	(10)	(11)	(12)	(13)	(14)	(15)	(16)	(17)	(18)	(19)	(20)	(21)	(22)																				
			Multipliers λ_{mk}				$a_{0k} = \Sigma [col. 13.] \times \lambda_{mk}$																					$\frac{c_l c}{b}$	$\frac{c_l c}{b}$	$\frac{c_l c}{b}$	$\frac{c_l c}{b}$	$\frac{c_l c}{b}$	$\frac{c_l c}{b}$	$\frac{c_l c}{b}$	$\frac{c_l c}{b}$	$\frac{c_l c}{b}$	$\frac{c_l c}{b}$										
$\frac{2y}{b}$	y_m	(Approx) $\frac{2y}{b}$	$\frac{k}{10}$	$\frac{9}{10}$	8	7	6	5	4	3	2	1	$\frac{\Sigma(3 \times 4)}{10}$	$\frac{a_c}{\delta}$	a	a_i	a_e	c_l	$\frac{c_l c}{b}$	$\frac{c_l c}{b}$	$\frac{c_l c}{b}$	$\frac{c_l c}{b}$	$\frac{c_l c}{b}$	$\frac{c_l c}{b}$																							
1st Approximation																																															
0	0	0.261	143.239	-58.533	0	-6.950	0	-2.865	0	-1.804	0	-1.468	5.97	0.0008	10.00	5.98	4.02	1.794	0.1587	0.275																											
0.1564	0	.248	-115.624	145.025	-67.298	0	-10.158	0	-4.840	0	-3.394	0	4.43	.0015	9.86	4.45	5.41	1.868	1.438	.269																											
0.3090	0	.222	0	-64.802	150.611	-67.157	0	-9.916	0	-4.968	0	-3.768	3.64	.0031	9.70	3.68	6.02	1.925	1.283	.249																											
0.4540	-0.0477	.195	-12.384	0	-62.917	160.761	-72.472	0	-10.926	0	-5.812	0	3.77	-.0068	9.50	3.69	5.81	1.904	1.155	.220																											
0.5878	.9112	.154	0	-8.320	0	-65.803	177.054	-82.083	0	-13.134	0	-7.713	2.40	.3154	9.27	6.19	3.08	1.643	1.027	.169																											
0.7071	.1876	.107	-4.051	0	-7.372	0	-71.743	202.571	-97.965	0	-17.388	0	-1.25	-.0878	9.02	-1.19	9.21	1.078	.0914	.099																											
0.8090	-0.0611	.085	0	-2.880	0	-7.208	0	-81.434	243.694	-125.537	0	-26.635	.05	-.0117	8.74	-0.09	8.83	1.049	.0817	.086																											
0.8910	0	.068	-1.638	0	-2.371	0	-7.370	0	-96.962	315.512	-180.528	0	.55	-.0122	8.47	.70	7.77	.942	.0739	.070																											
0.9510	0	.064	0	-1.062	0	-2.016	0	-7.599	0	-122.880	463.533	-329.976	2.75	-.0086	8.23	2.71	5.52	.724	.0681	.049																											
0.9877	0	.037	-0.459	0	-0.620	0	-1.491	0	-7.089	0	-167.045	915.651	11.39	.0065	8.06	11.47	-3.41	-1.178	.0590	-.010																											
$\frac{2y}{b}$	$\frac{c_l c}{b} = \Sigma(2 \times 3)$	$\frac{c_l c}{b} = 0.147$	$c_l^* = \left(\frac{c_l c}{b}\right) / \left(\frac{c}{b}\right)$																				$\frac{2y}{b} - 0$	$\frac{2y}{b} + 0$																							
0.6			Outboard end of flap span																				9.25	9.25	9.25	9.25	9.25	9.25	9.25	9.25	9.25	9.25	9.25	9.25	9.25	9.25	9.25	9.25	9.25	9.25	9.25	9.25	9.25	9.25	9.25		
			Inboard end of unfliapped span																				9.25	9.25	9.25	9.25	9.25	9.25	9.25	9.25	9.25	9.25	9.25	9.25	9.25	9.25	9.25	9.25	9.25	9.25	9.25	9.25	9.25	9.25	9.25	9.25	9.25
2nd Approximation																																															
0	0	0.277	143.239	-58.533	0	-6.950	0	-2.865	0	-1.804	0	-1.468	5.95	0.0006	10.00	5.96	4.04	1.786	0.1587	0.276																											
0.1564	0	.264	-115.624	145.025	-67.298	0	-10.158	0	-4.840	0	-3.394	0	4.72	.0015	9.86	4.74	5.12	1.843	1.438	.265																											
0.3090	0	.242	0	-64.802	150.611	-67.157	0	-9.916	0	-4.968	0	-3.768	4.30	.0031	9.70	4.34	5.36	1.867	1.293	.241																											
0.4540	-0.0477	.213	-12.384	0	-62.917	160.761	-72.472	0	-10.926	0	-5.812	0	4.48	-.0068	9.50	4.40	5.10	1.843	1.155	.213																											
0.5878	.9112	.165	0	-8.320	0	-65.803	177.054	-82.083	0	-13.134	0	-7.713	2.80	.3154	9.27	6.58	2.68	1.607	1.027	.165																											
0.7071	.1876	.108	-4.051	0	-7.372	0	-71.743	202.571	-97.965	0	-17.388	0	-2.25	-.0878	9.02	-1.19	10.21	1.175	.0914	.107																											
0.8090	-0.0611	.086	0	-2.880	0	-7.208	0	-81.434	243.694	-125.537	0	-26.635	-.03	-.0117	8.74	-1.17	8.91	1.056	.0817	.088																											
0.8910	0	.063	-1.638	0	-2.371	0	-7.370	0	-96.962	315.512	-180.528	0	.52	-.0122	8.47	.67	7.80	.944	.0739	.070																											
0.9510	0	.051	0	-1.062	0	-2.016	0	-7.599	0	-122.880	463.533	-329.976	2.51	-.0086	8.23	2.47	5.76	.746	.0681	.051																											
0.9877	0	.029	-0.459	0	-0.620	0	-1.491	0	-7.089	0	-167.045	915.651	4.84	.0065	8.06	4.92	3.14	.481	.0590	.028																											
$\frac{2y}{b}$	$\frac{c_l c}{b} = \Sigma(2 \times 3)$	$\frac{c_l c}{b} = 0.156$	$c_l^* = \left(\frac{c_l c}{b}\right) / \left(\frac{c}{b}\right)$																				$\frac{2y}{b} - 0$	$\frac{2y}{b} + 0$																							
0.6			Outboard end of flap span																				9.25	9.25	9.25	9.25	9.25	9.25	9.25	9.25	9.25	9.25	9.25	9.25	9.25	9.25	9.25	9.25	9.25	9.25	9.25	9.25	9.25	9.25	9.25		
			Inboard end of unfliapped span																				9.25	9.25	9.25	9.25	9.25	9.25	9.25	9.25	9.25	9.25	9.25	9.25	9.25	9.25	9.25	9.25	9.25	9.25	9.25	9.25	9.25	9.25	9.25	9.25	



TABLE XI.- CALCULATION OF WING COEFFICIENTS

FOR EXAMPLE WING

$$\left[A = \underline{9.021}; \alpha_s = \underline{10.00} \right]$$

(1)	(2)	(3)	(4)	(5)
$\frac{2y}{b}$	Multipliers η_{ms}	$\frac{c_{l'c}}{b}$ (table X)	α_i (table X)	$\frac{c_{l'c}}{b} \times \alpha_i$ (3) \times (4)
0	0.05236	0.277	5.96	1.651
.1564	.20686	.264	4.74	1.251
.3090	.09960	.242	4.34	1.050
.4540	.18659	.213	4.40	.937
.5878	.04870	.165	6.59	1.087
.7071	.14130	.108	-1.19	-.129
.8090	.06290	.086	-.17	-.015
.8910	.09508	.068	.67	.046
.9511	.03236	.051	2.47	.126
.9877	.03276	.029	4.92	.143
.6 - 0	.00589	.156	7.30	.114
.6 + 0	.03560	.156	-4.72	-.736

$$C_L = A \sum (2) \times (3) = 1.599$$



$$C_{D_i} = \frac{A \sum (2) \times (5)}{57.3} = 0.1017$$

TABLE XII — CALCULATION OF ASYMMETRICAL LIFT DISTRIBUTION FOR EXAMPLE WING WITH 0.6 SPAN FLAPS

(1)	(2)	(3)	(4)	(5)	(6)	(7)	(8)	(9)	(10)	(11)	(12)	(13)	(14)	(15)	(16)	(17)	(18)	(19)	(20)	(21)	(22)	(23)	(24)	(25)			
$\frac{2\gamma}{b}$	γ_m	$\frac{c_c}{b}$ (Approx) $\frac{2\gamma}{b} \cdot \frac{1}{2} \sum_{k=1}^n \frac{1}{k}$	Multipliers β_{mk}		$\alpha_{uk} = \sum_{j=1}^k \beta_{mj}$ for $19 \leq k \leq 10$		$\alpha_{uk} = \sum_{j=1}^k \beta_{mj}$ for $10 \leq k \leq 1$		σ_{uk}	$\sum_{k=1}^{10} \sigma_{uk}$	12	11	10	$\frac{c_c}{b}$ Reverse $\sum_{k=1}^n \frac{1}{k}$	$\frac{a_c}{\delta_c}$ $\frac{a_c}{\delta_c}$	$\frac{a_c}{\delta_c}$ $\frac{a_c}{\delta_c}$	$\frac{a_c}{\delta_c}$ $\frac{a_c}{\delta_c}$	a $(s_2 + \epsilon)$ $(s_2 + \epsilon)$	a_i $(15) \cdot (18)$	$\Delta \sigma \delta$ (a)	a_e $(19) \cdot (20) \cdot (21)$	c_l (23)	$\frac{c_l}{b}$ $(23) \cdot (24)$	Check $\frac{c_l}{b}$			
			k/19	18	17	16	15	14																	13	12	11
-0.6		$\frac{2\gamma}{b} \left(\frac{c_c}{b} \right) = 2(2)(3)$ = 0.1537																									
.988	0	0.0278	915.651	166.985	0	-7.019	0	-1.401	0	-486	0	-230	0.0301	4.42	0.0063	0.0002	0.08	7.49	4.50	-0.2	3.01	1.513	0.1016	0.1537			
.951	0	.0492	329.859	463.533	-122.749	0	-7.438	0	-1.792	0	-701	0	.0531	2.25	-0.0036	0	-0.4	7.68	2.21	-0.2	5.49	.473	.0681	.0492			
.891	0	.0682	0	-180.336	315.512	-96.737	0	-7.073	0	-1.920	0	-819	.0710	.51	.0120	.0002	.15	7.96	.86	-0.2	7.32	.895	.0739	.0681			
.809	.0511	.0838	-26.374	0	-125.246	243.694	-81.067	0	-6.680	0	-1.977	0	.0888	-15	-0.0117	0	-1.4	8.28	-29	-0.2	8.59	1.025	.0817	.0837			
.707	.1876	.1053	0	-17.020	0	-97.524	202.571	-71.139	0	-6.391	0	-2.026	.1103	-2.39	.0876	.0002	1.05	8.61	-1.34	-0.2	9.97	1.162	.0914	.1053			
.588	.9112	.1627	-7.246	0	-12.604	0	-81.392	177.054	-64.735	0	-6.228	0	.1671	2.75	.3154	0	3.79	8.94	6.54	-0.2	2.42	1.584	.1027	.1627			
.454	-.0477	.2109	0	-5.166	0	-10.126	0	-71.296	160.761	-60.725	0	-6.192	.2146	4.41	.0030	.0001	-0.8	9.24	4.33	-0.1	4.90	1.826	.1155	.2109			
.309	.2104	.2404	-2.958	0	-4.022	0	-8.596	0	-64.817	150.611	-58.514	0	.2431	4.23	.0030	.0001	.04	9.52	4.27	-0.1	5.26	1.859	.1293	.2404			
.156	0	.2635	0	-2.241	0	-3.322	0	-7.604	0	-60.768	145.025	-57.812	.2650	4.78	.0009	.0006	.02	9.77	4.78	0	4.99	1.833	.1438	.2635			
0	0	.2767	-1.468	0	-1.804	0	-2.865	0	-6.950	0	-5.833	143.239	.2767	5.88	.0003	.0003	.01	10.00	5.89	0	4.11	1.743	.1587	.2766			
.156	0	.2650	0	-1.153	0	-1.518	0	-2.554	0	-6.530	0	-57.812	.2635	4.81	.0006	.0009	.02	9.95	4.83	0	5.12	1.843	.1438	.2650			
.309	0	.2431	-.810	0	-.946	0	-1.319	0	-2.340	0	-6.288	0	.2404	4.30	.0001	.0030	.04	9.87	4.34	.01	5.52	1.880	.1293	.2431			
.454	0	.2146	0	-.646	0	-.800	0	-1.176	0	-2.192	0	-6.192	.2109	4.52	.0003	-.0071	-.08	9.76	4.44	.01	5.31	1.858	.1155	.2146			
.588	0	.1671	-.467	0	-.530	0	-.691	0	-1.068	0	-2.092	0	.1627	2.87	0	.3154	3.81	9.61	6.68	.02	2.91	1.826	.1027	.1670			
.707	0	.1103	0	-.368	0	-.441	0	-.604	0	-.981	0	-2.026	.1053	-2.20	.0002	.0876	1.06	9.42	-1.14	.02	10.54	1.207	.0914	.1103			
.809	0	.0888	-.261	0	-.291	0	-.366	0	-.528	0	-.903	0	.0838	.12	0	-0.117	-1.4	9.21	-0.2	.02	9.21	1.087	.0817	.0888			
.891	0	.0710	0	-.192	0	-.225	0	-.297	0	-.452	0	-.819	.0662	.83	.0002	.0120	.15	8.98	.98	.02	7.98	.961	.0739	.0710			
.951	0	.0531	-.118	0	-.130	0	-.161	0	-.224	0	-.361	0	.0492	2.71	0	-.0036	-.04	8.77	2.68	.02	6.07	.778	.0681	.0530			
.988	0	.0301	0	-.060	0	-.069	0	-.090	0	-.133	0	-.230	.0278	5.07	.0002	.0063	.08	8.63	5.15	.02	3.46	.514	.0580	.0301			
$\frac{2\gamma}{b} \left(\frac{c_c}{b} \right) = 2(2)(4)$ = 0.1582																											
			$\frac{2\gamma}{b} / .988$.951	.891	.809	.707	.588	.454	.309	.156	0															
			k/1	2	3	4	5	6	7	8	9	10															



$\Delta a_e = \frac{E \cdot \epsilon}{2E} [(a-\alpha)_k - (a-\alpha)_{20-k}]$

TABLE XIII.- COEFFICIENTS USED TO OBTAIN
SUCCEEDING APPROXIMATIONS

$\frac{AE}{\eta}$	K	K_0	K_1	K_2	K_3
4	10.095	2.384	1.000	0.498	0.339
8	8.418	3.000	1.000	.401	.258
12	8.141	3.571	1.000	.338	.215



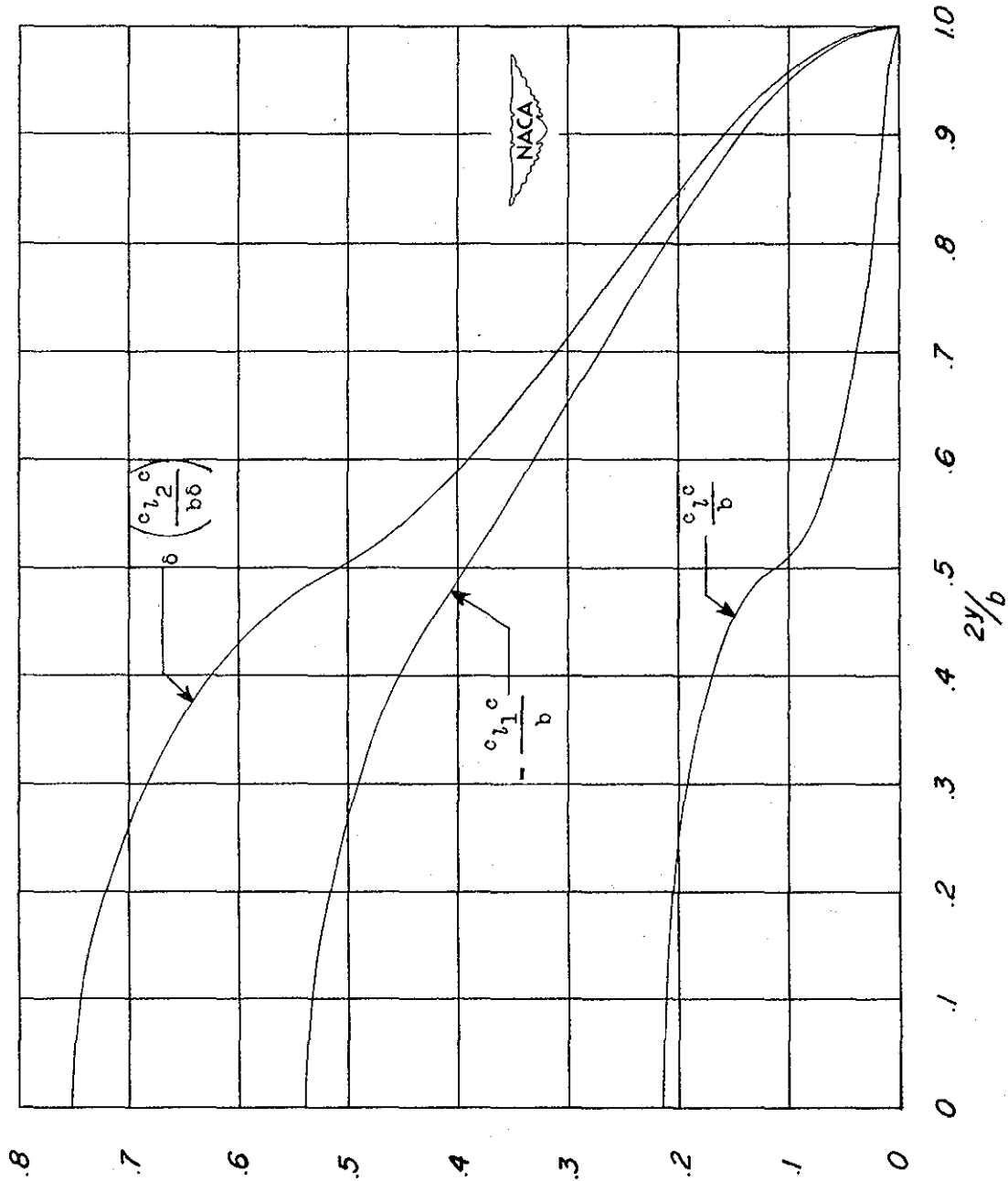
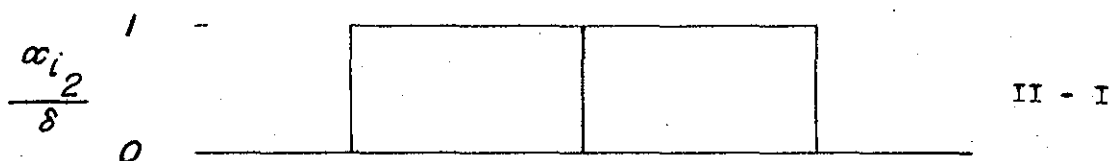
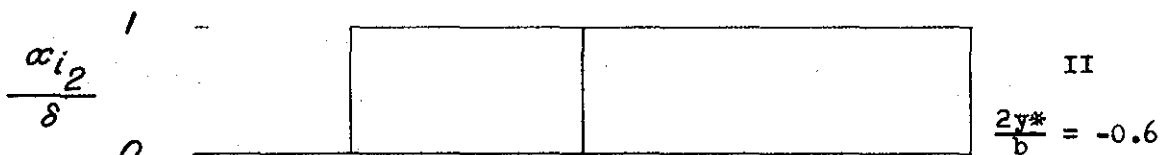


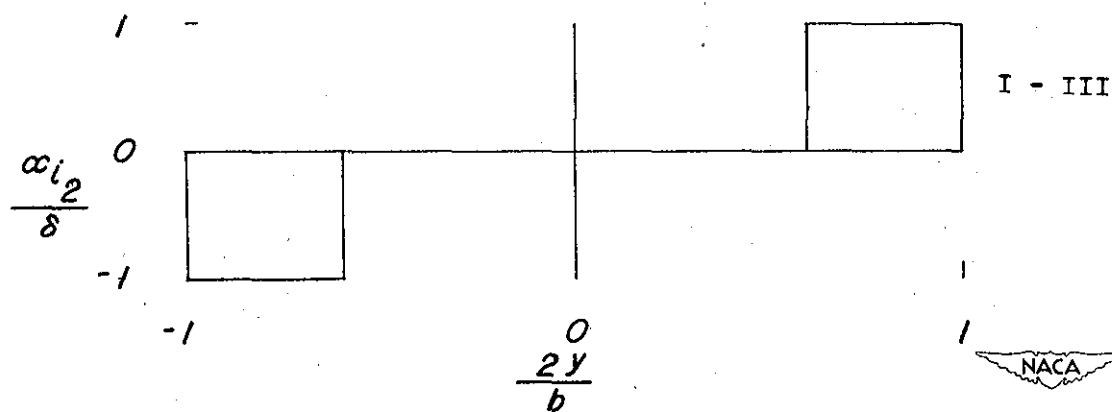
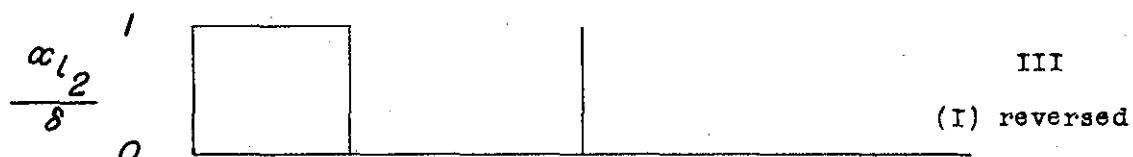
Figure 1.- Typical lift distributions for a wing with 0.5-span flaps.



(a) Asymmetrical distribution.



(b) Symmetrical distribution.



(c) Antisymmetrical distribution.

Figure 2.- Method of combining distributions of α_{i2}/δ .

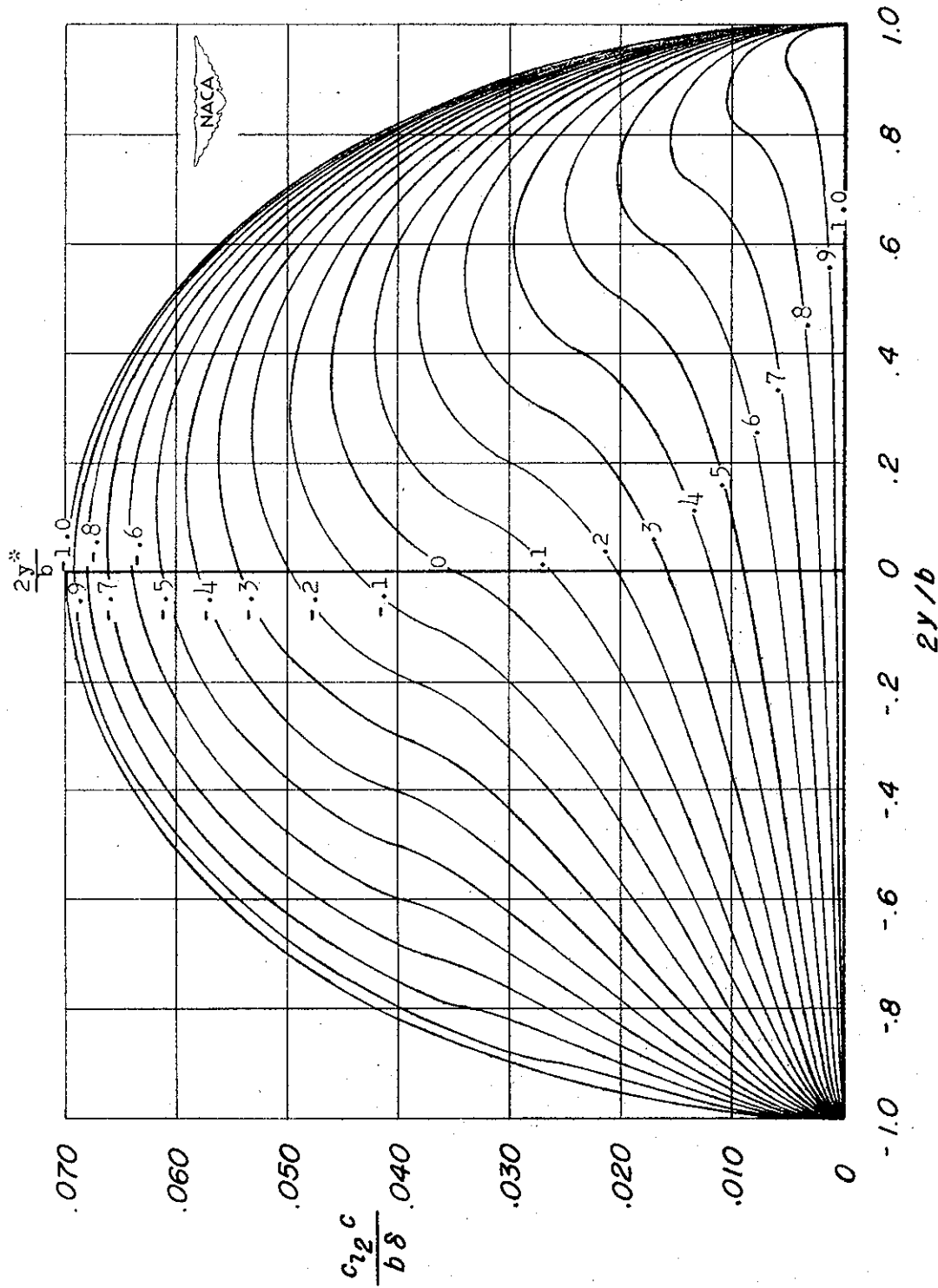


Figure 3.- Lift distribution per degree of discontinuity in induced angle of attack for various spanwise locations of the discontinuity $2y^*/b$.

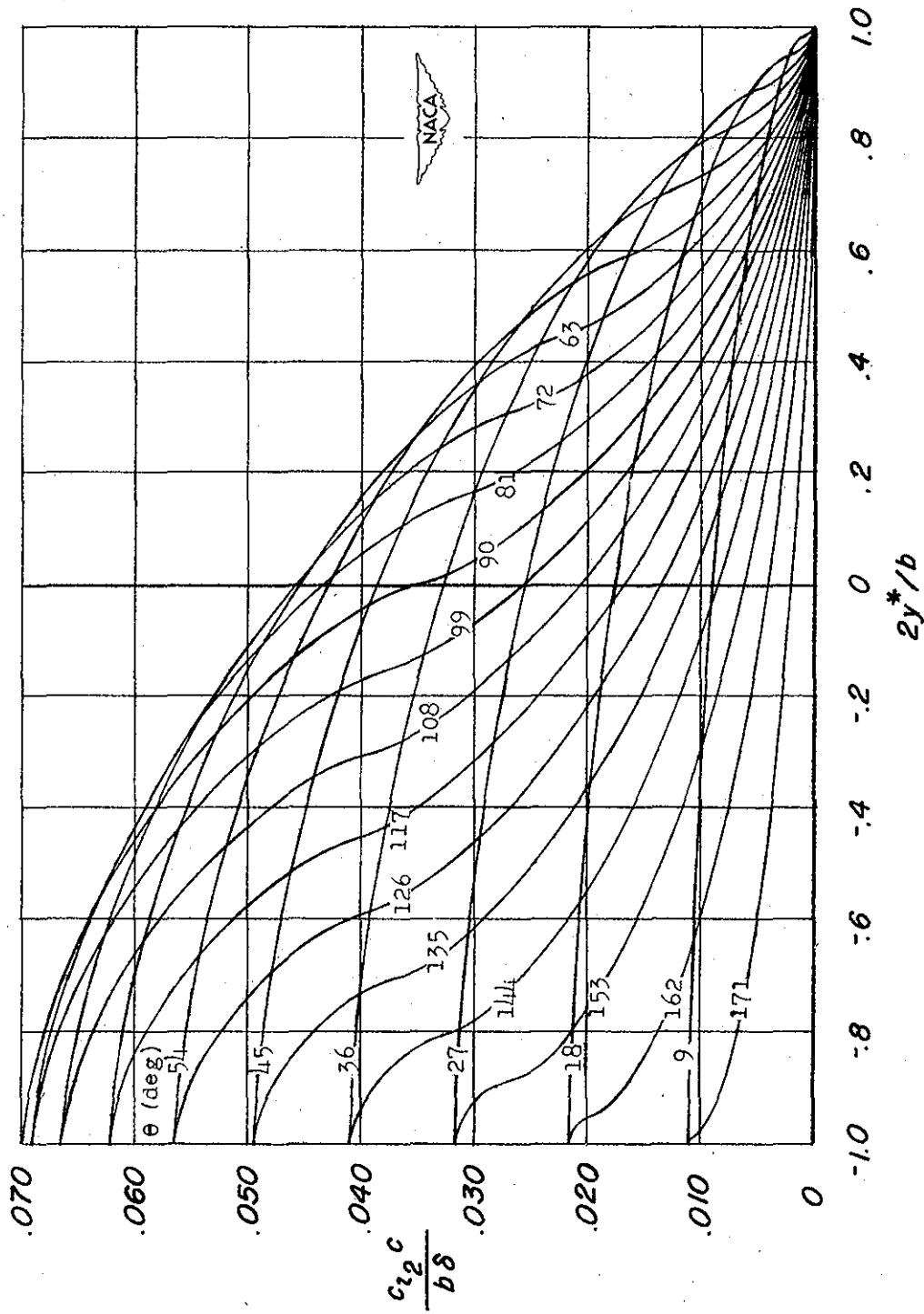


Figure 4.- Values of the lift distribution per degree of discontinuity in induced angle of attack as a function of the spanwise location of the discontinuity $2y^*/b$.

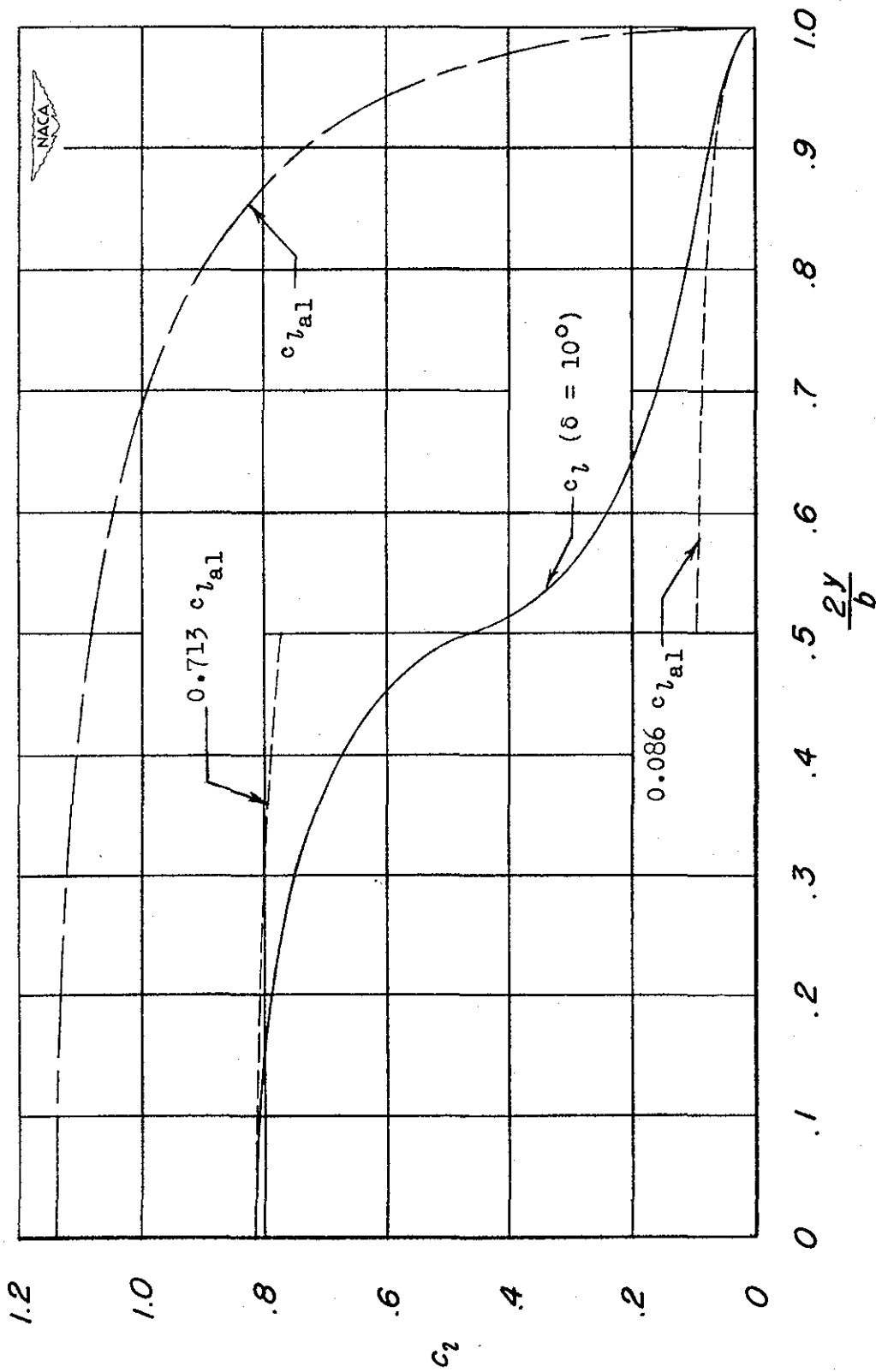


Figure 5.- Typical curves used to obtain factor for altering two-dimensional data.

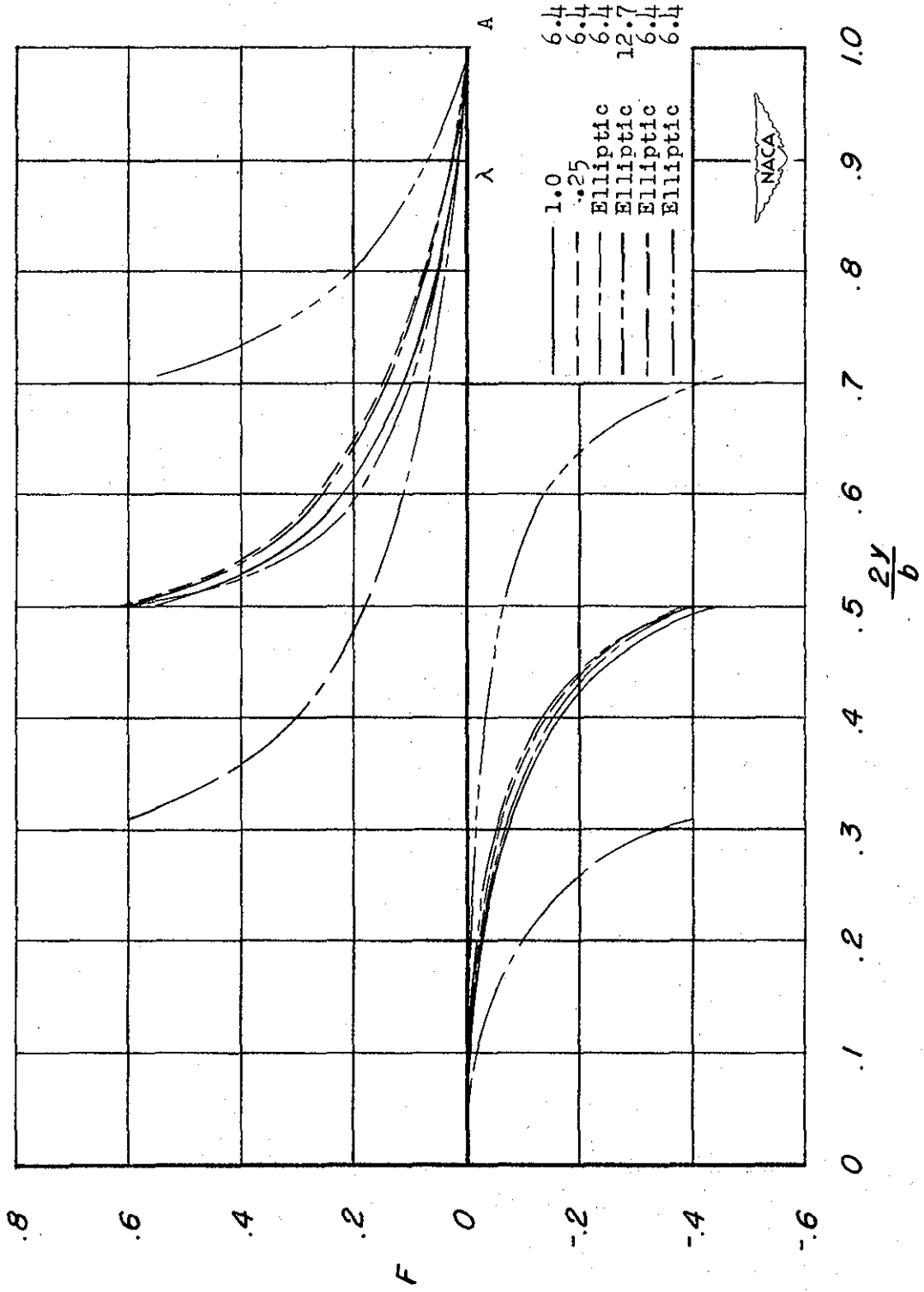


Figure 6.- Factor for altering two-dimensional data for several wings.

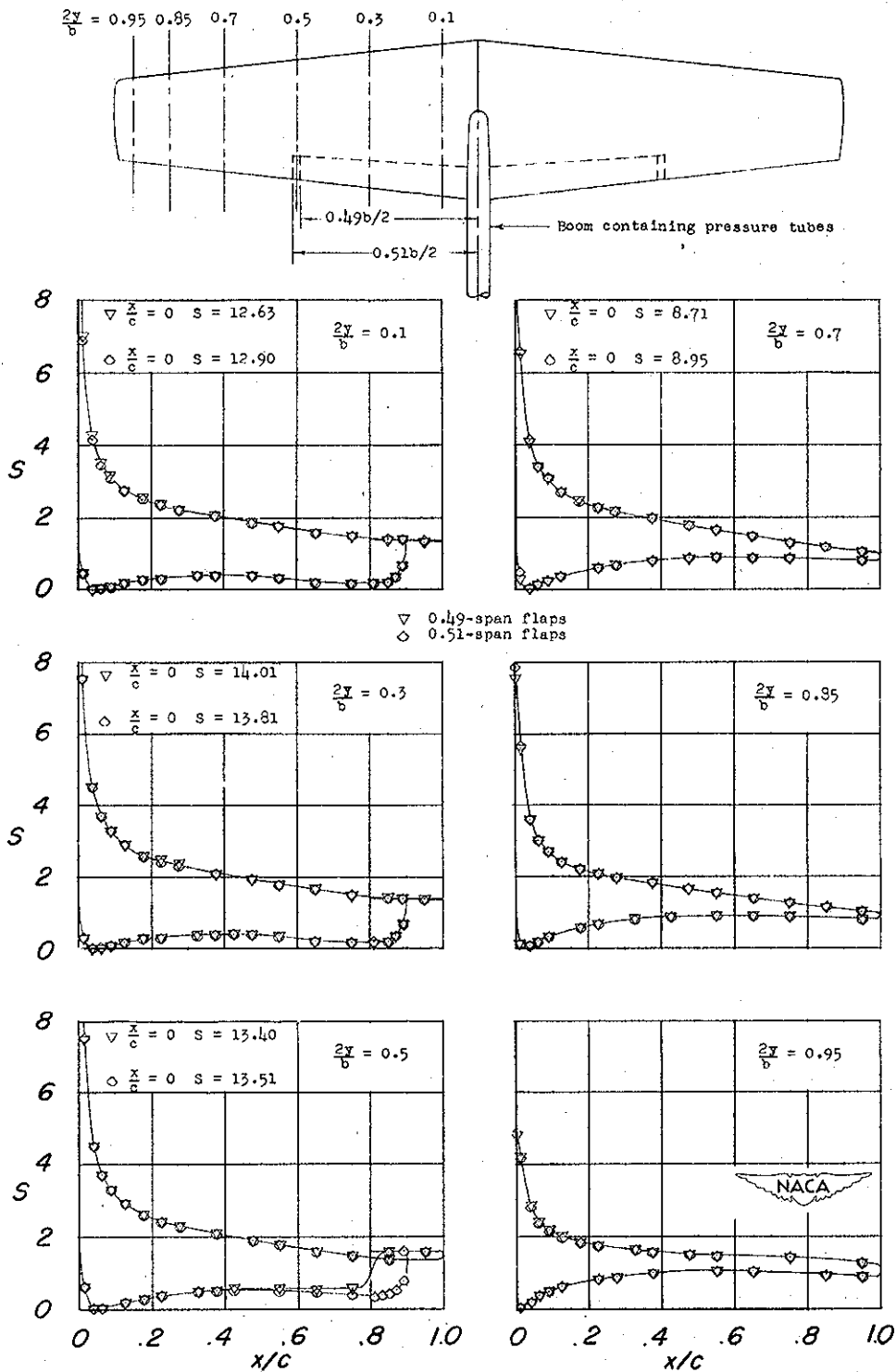
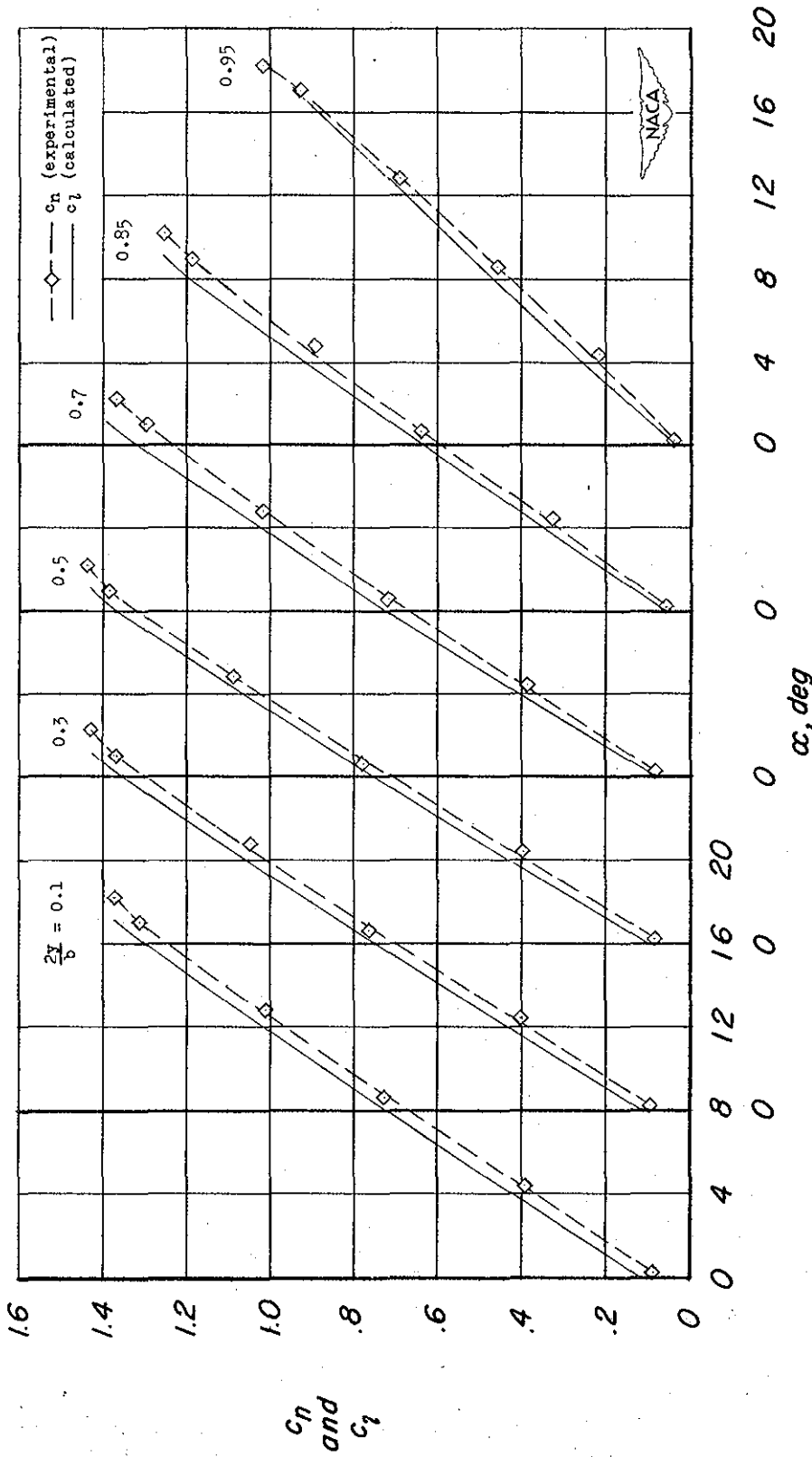
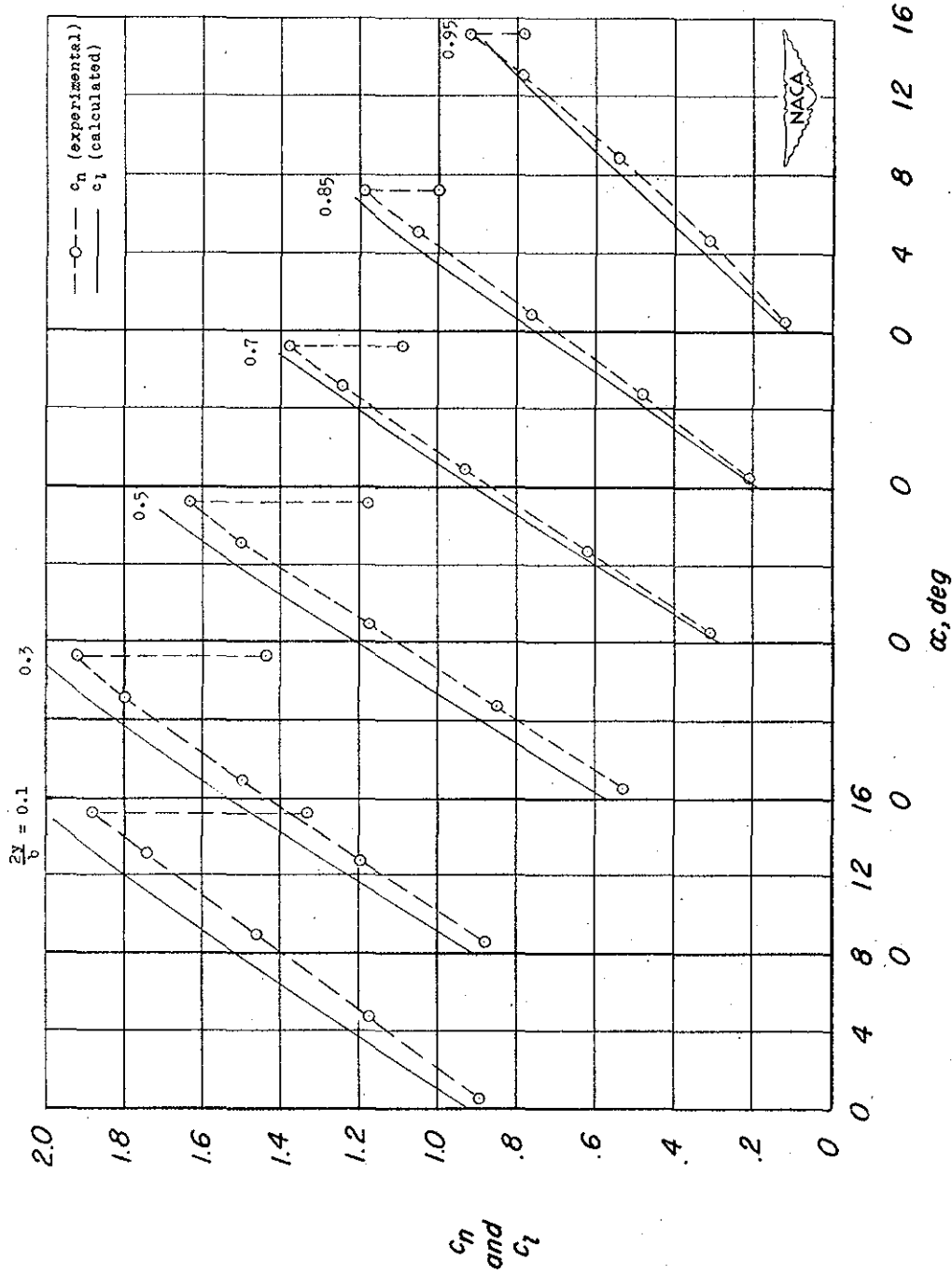


Figure 7.- Experimental pressure distributions at an angle of attack of 13.1° for a wing having NACA 64-210 airfoil sections, an aspect ratio of 6.0, a taper ratio of 0.5, and partial-span split flaps.



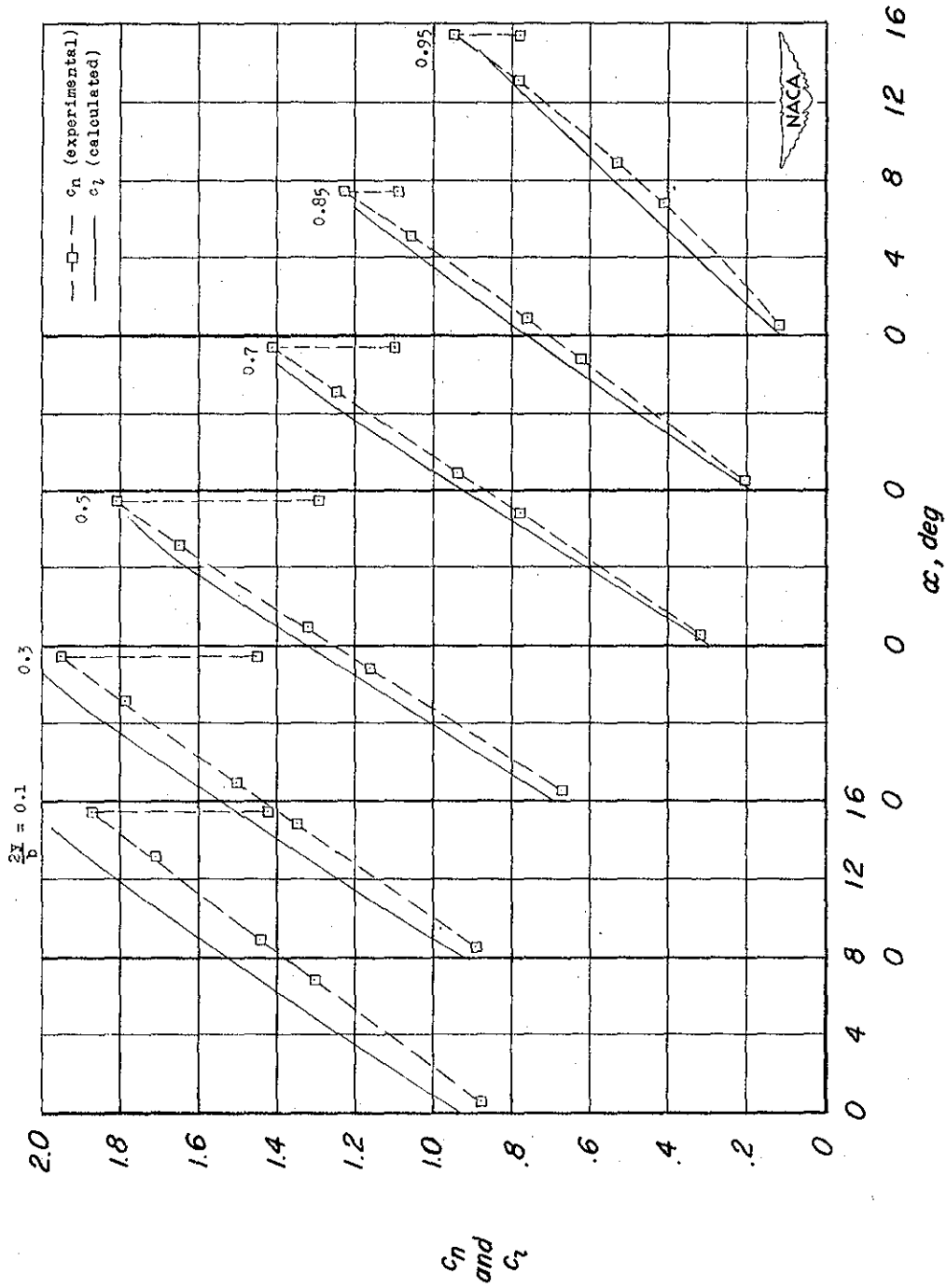
(a) Flaps neutral.

Figure 8.- Comparison of experimental and calculated section characteristics for a wing having NACA 64-210 airfoil sections, an aspect ratio of 6.0, and a taper ratio of 0.5.



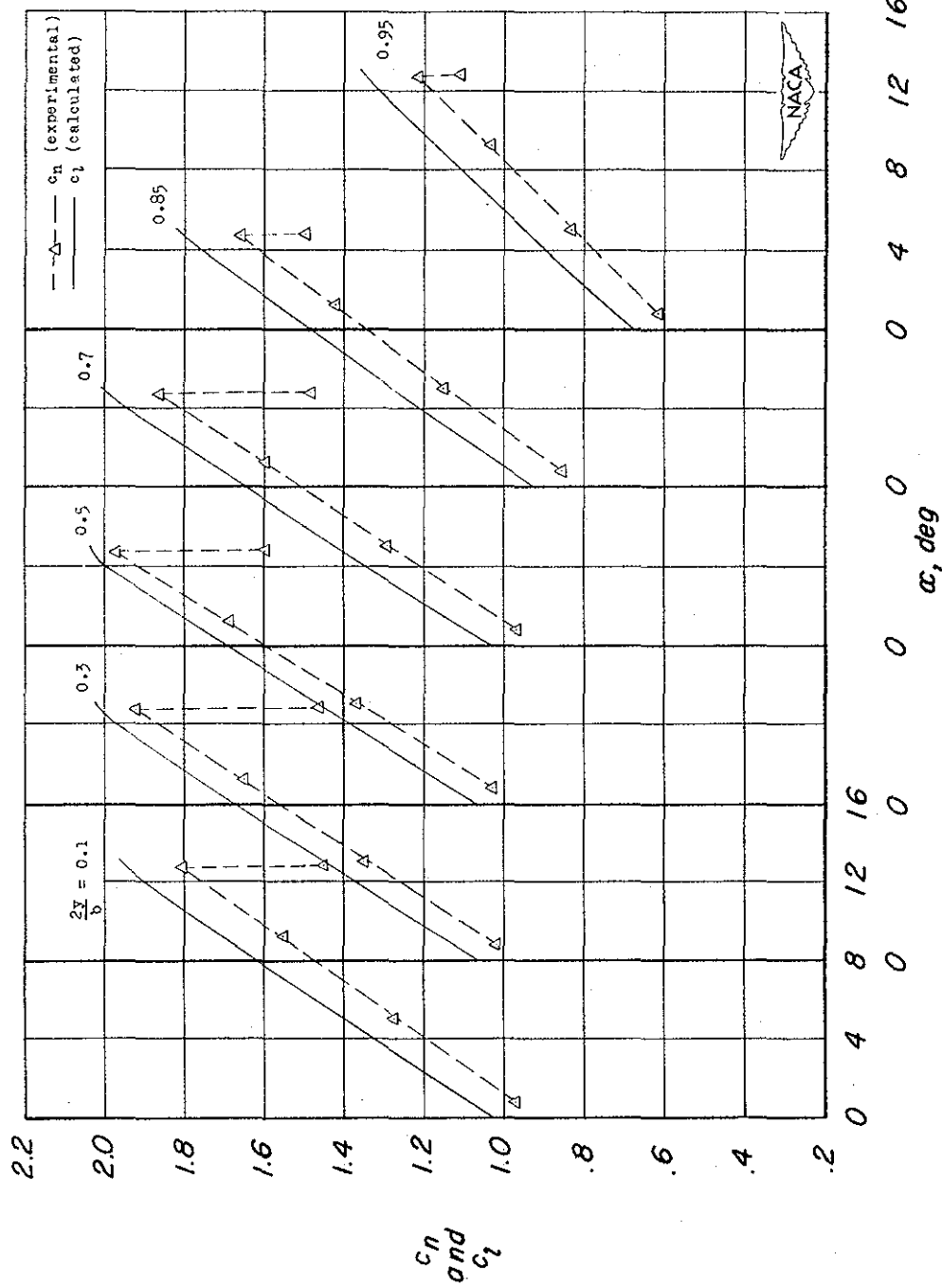
(b) 0.49-span split flaps.

Figure 8.- Continued.



(c) 0.51-span split flaps.

Figure 8.- Continued.



(d) Full-span split flaps.

Figure 8.- Concluded.

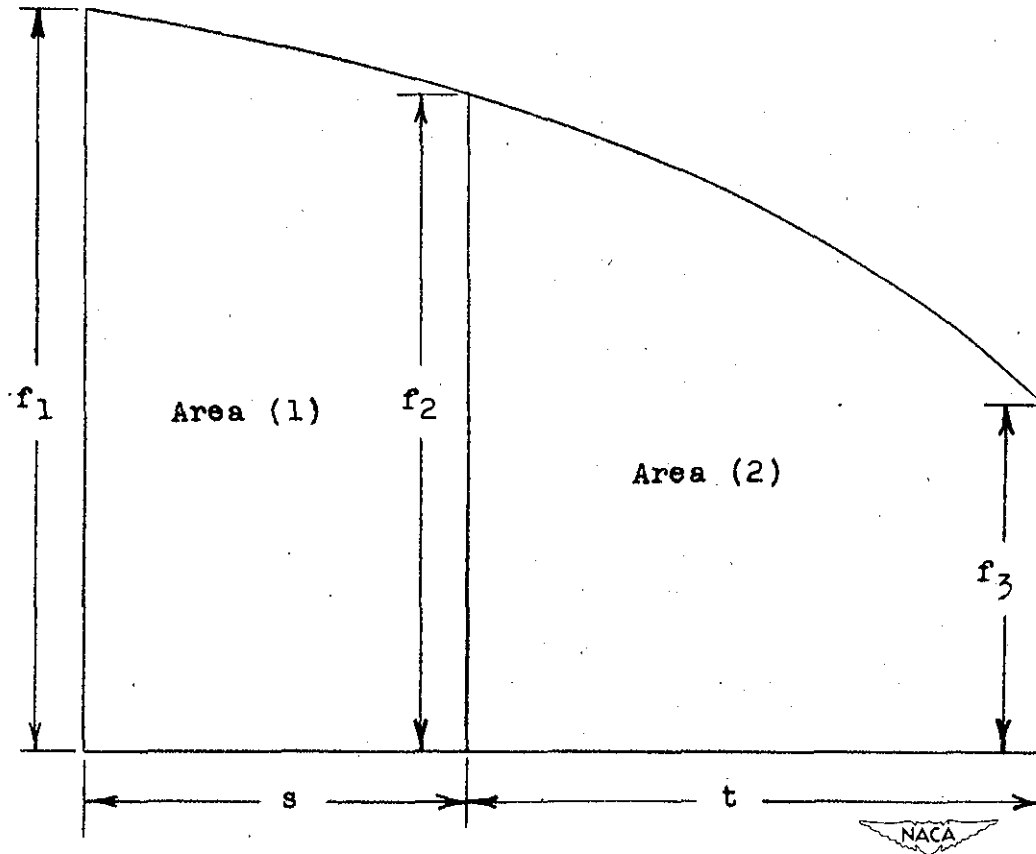


Figure 9.- Definition of symbols used in numerical integration for unequal increments in independent variable.

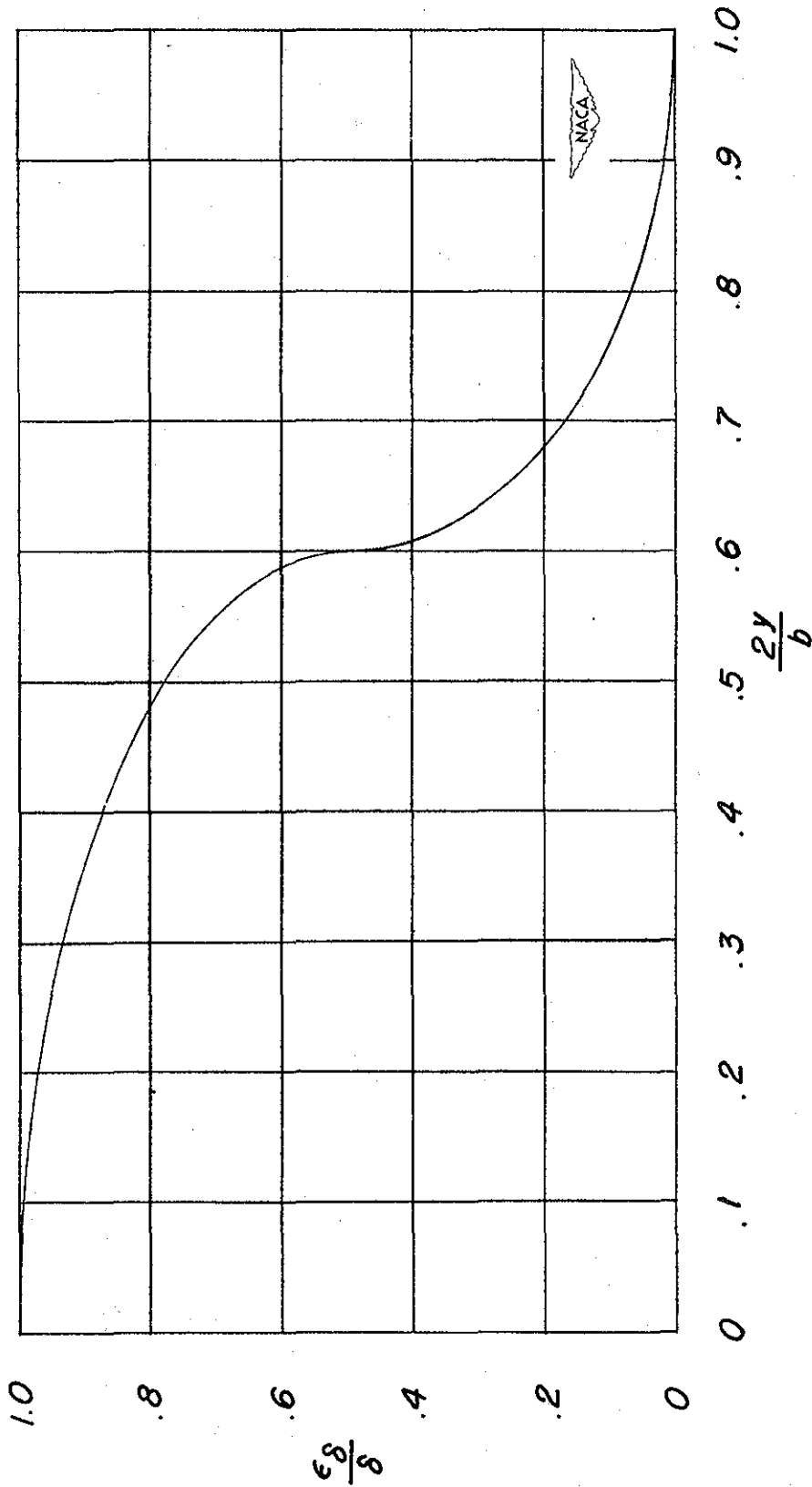


Figure 11.- Fairing of discontinuity due to flap deflection for initial approximation.

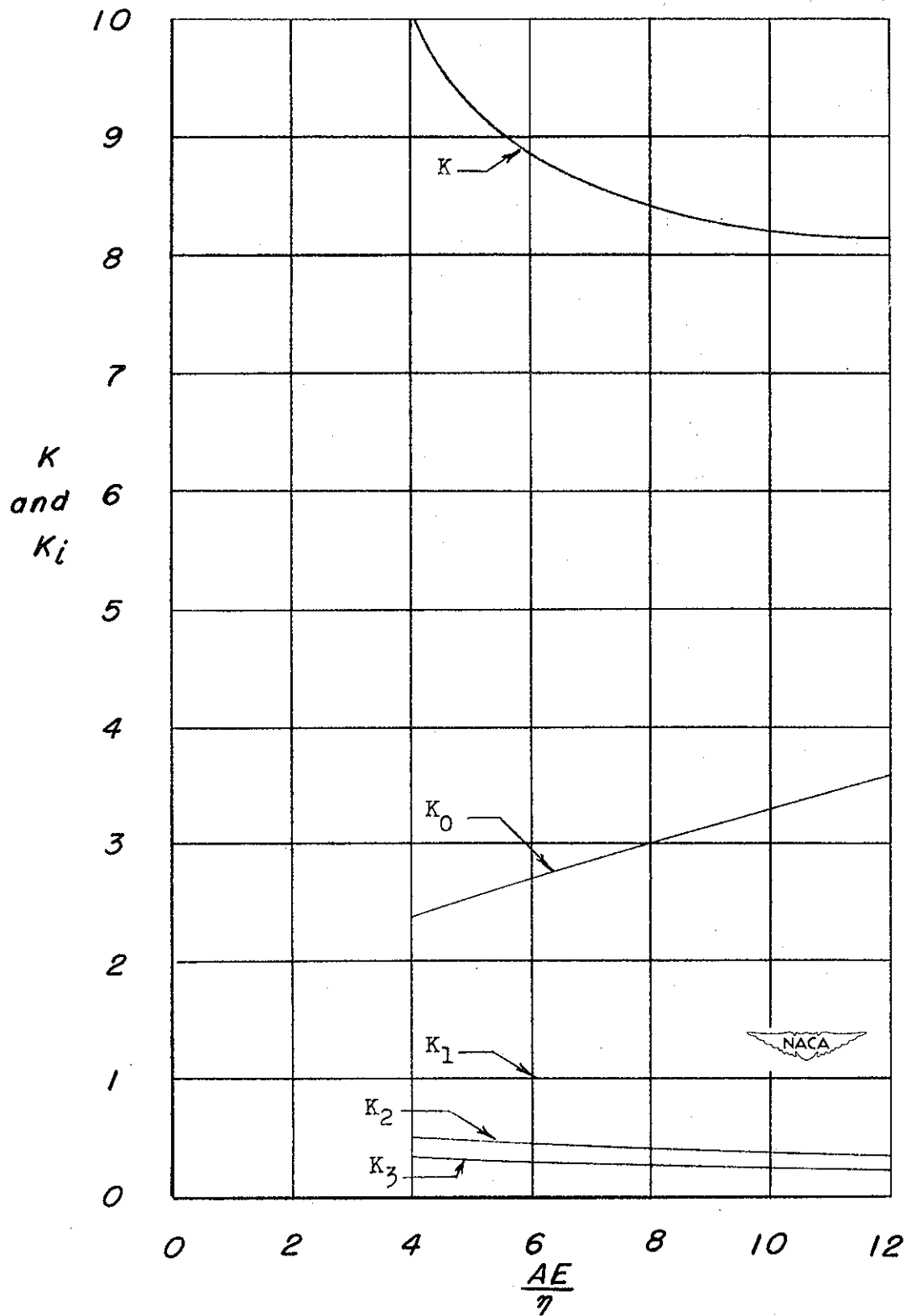
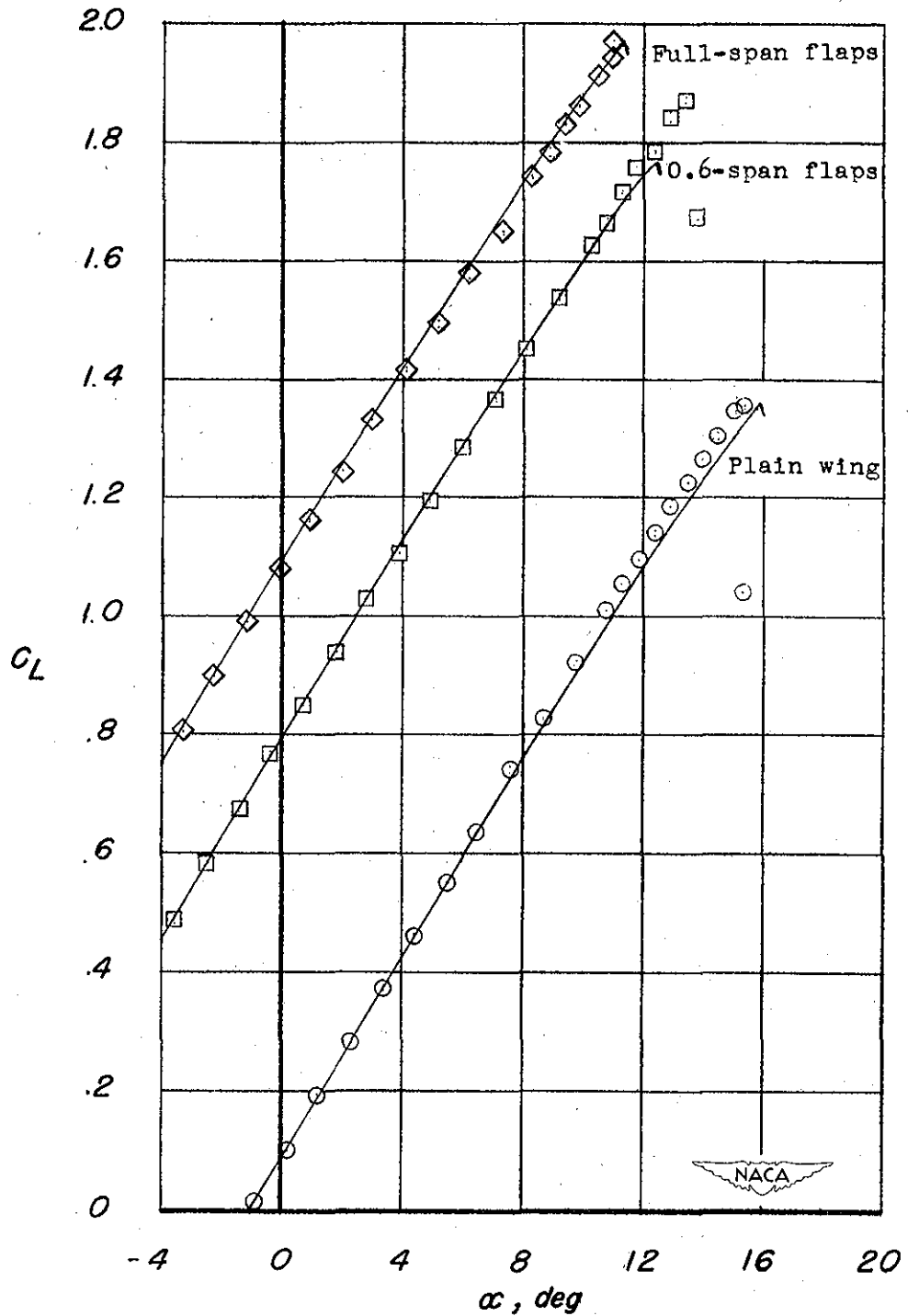
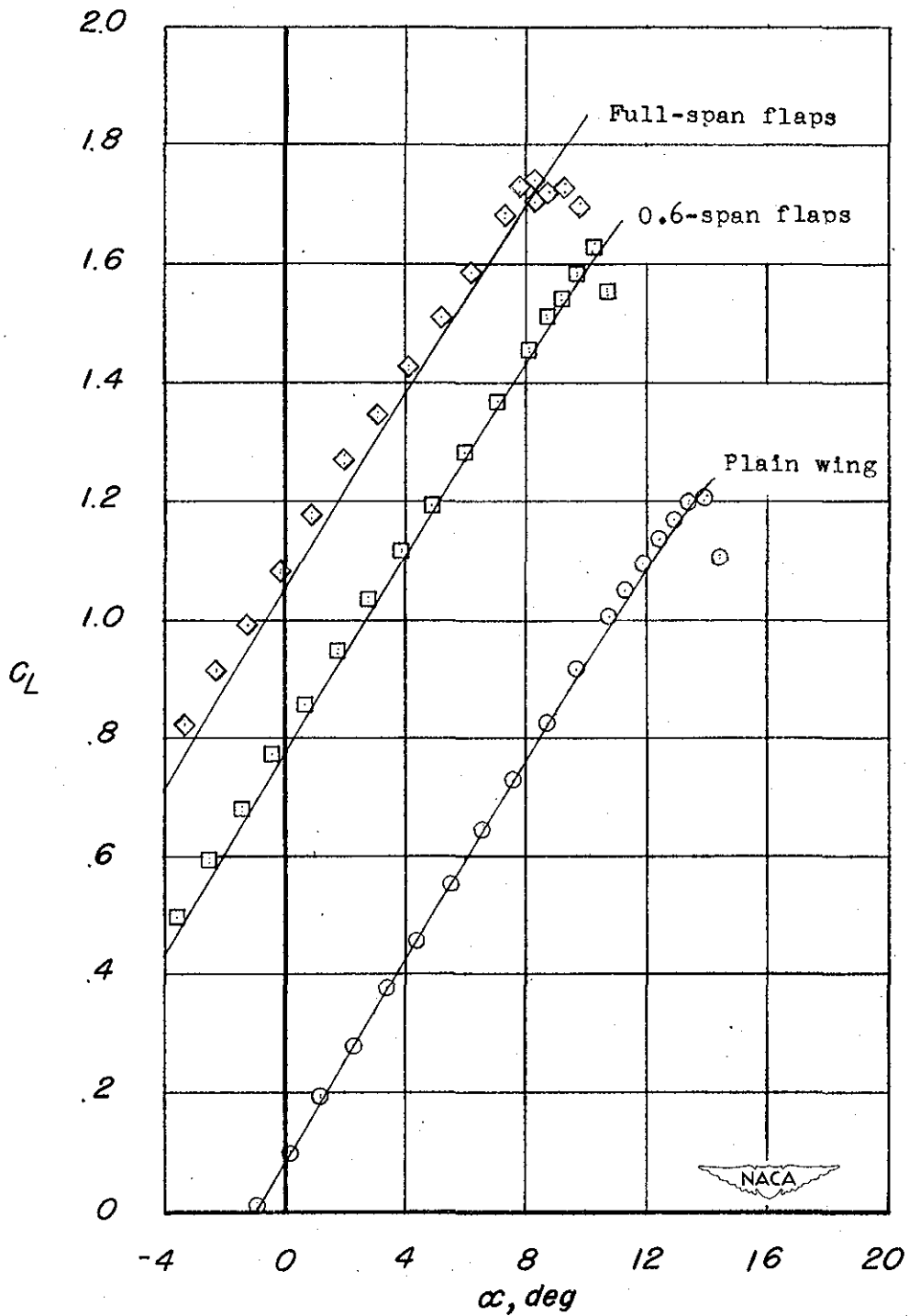


Figure 12.- Coefficients used to obtain succeeding approximations. $r = 20$.



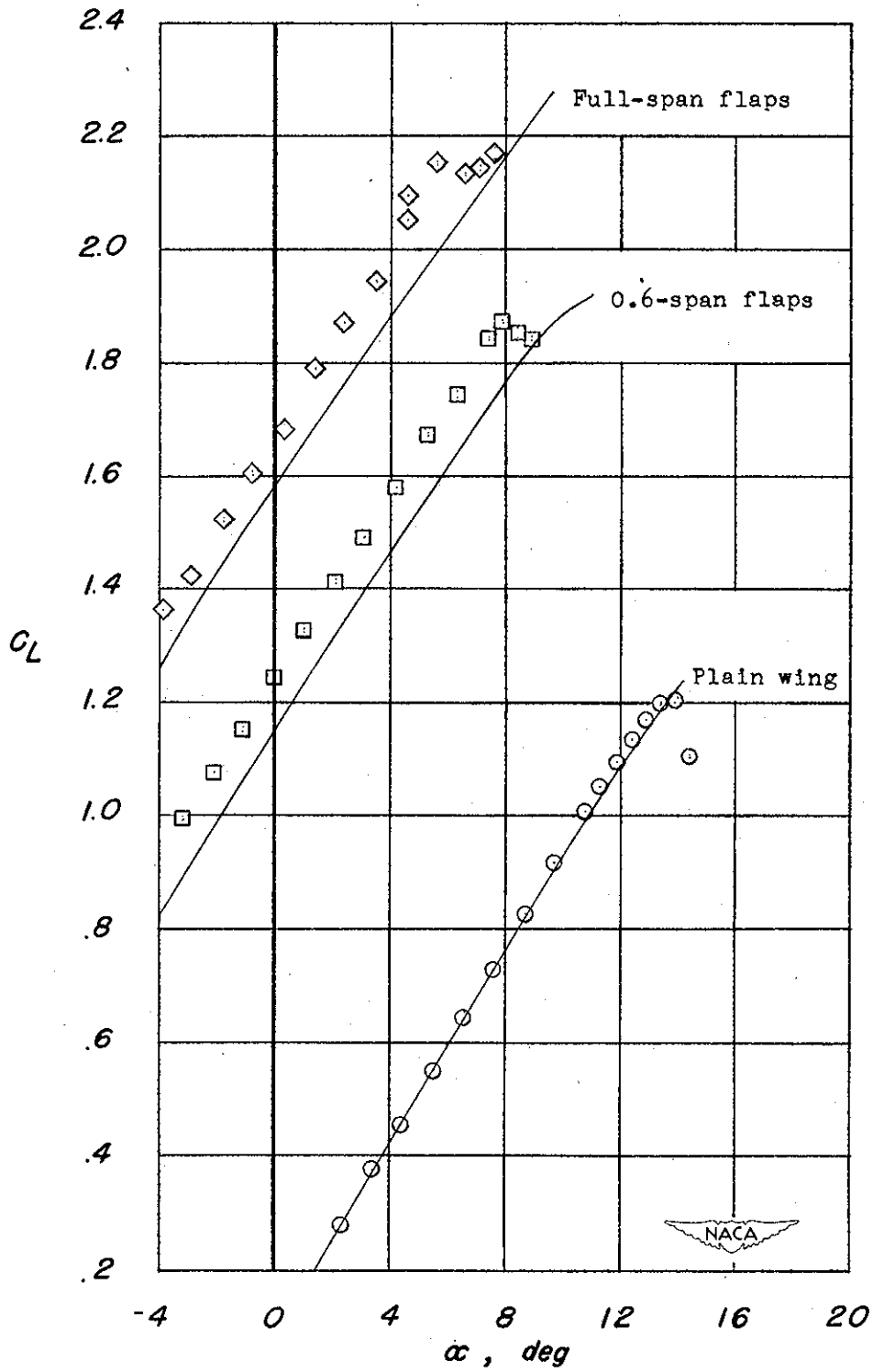
(a) NACA 64-210 sections; split flaps.

Figure 13.- Experimental and calculated lift curves for wings with and without flaps; aspect ratio, 9.021; taper ratio, 0.4; washout, 2° . Experimental points designated by symbols.



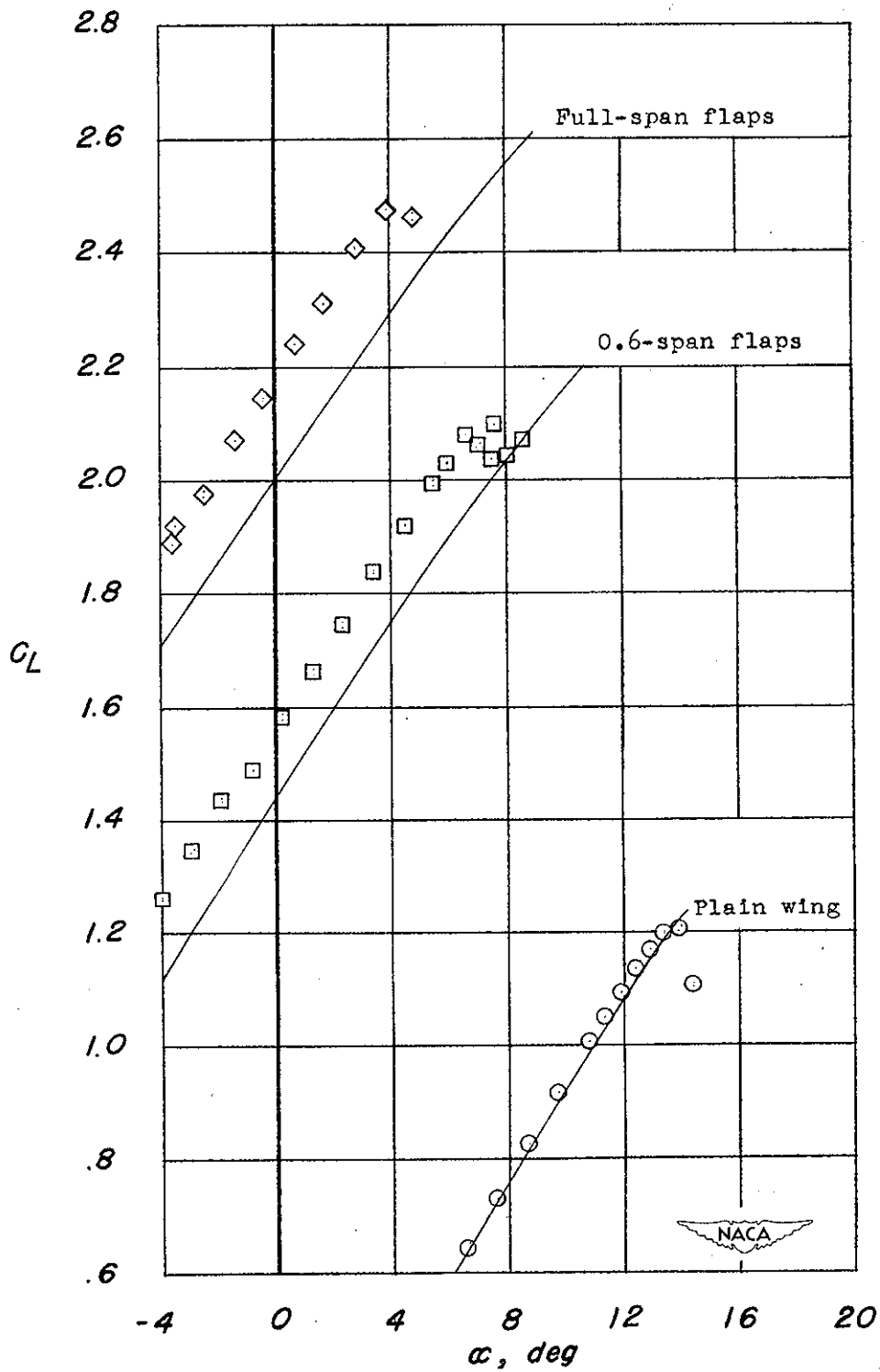
(b) NACA 65-210 sections; split flaps.

Figure 13.- Continued.



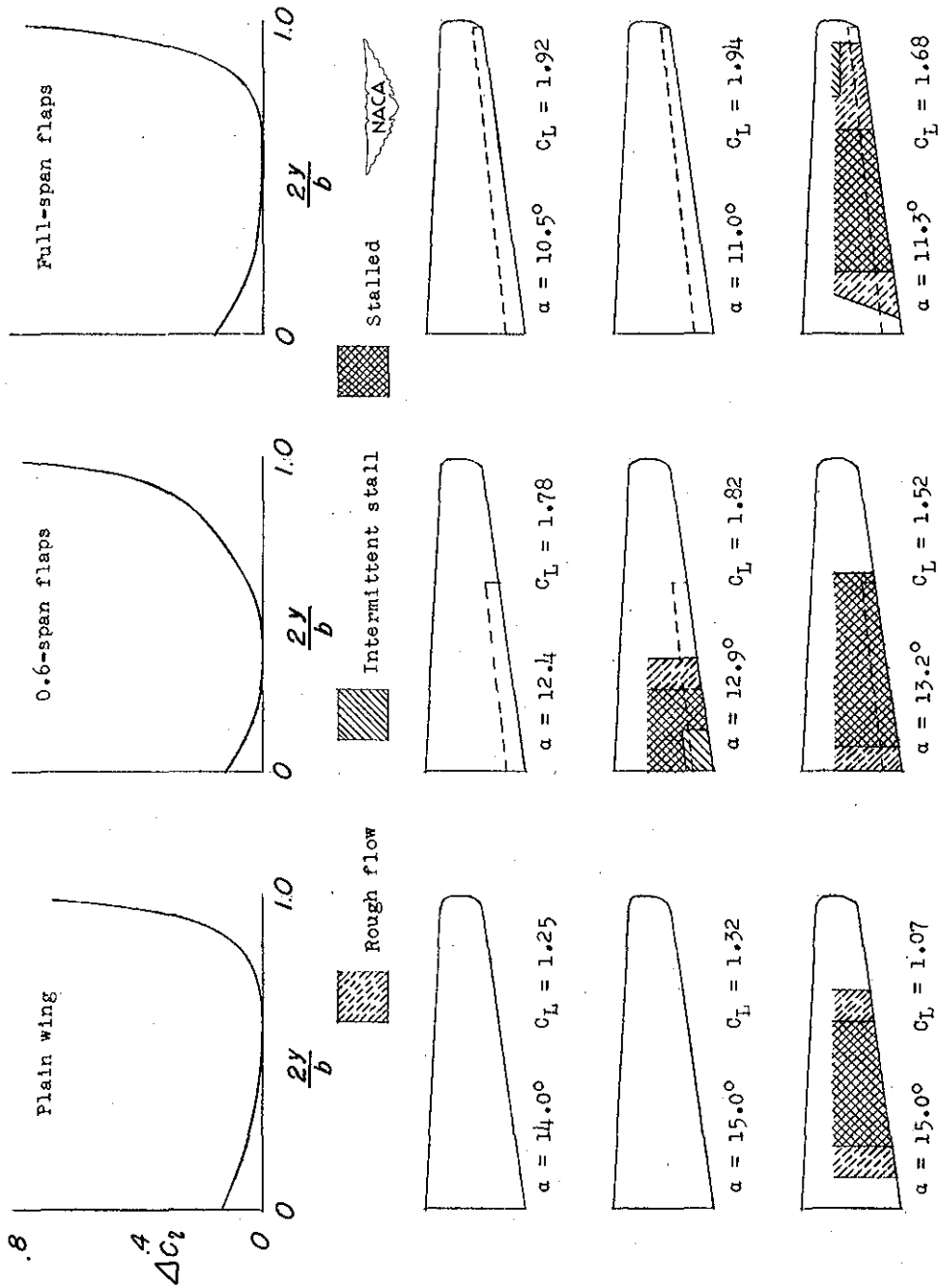
(c) NACA 65-210 sections; single slotted flaps.

Figure 13.- Continued.



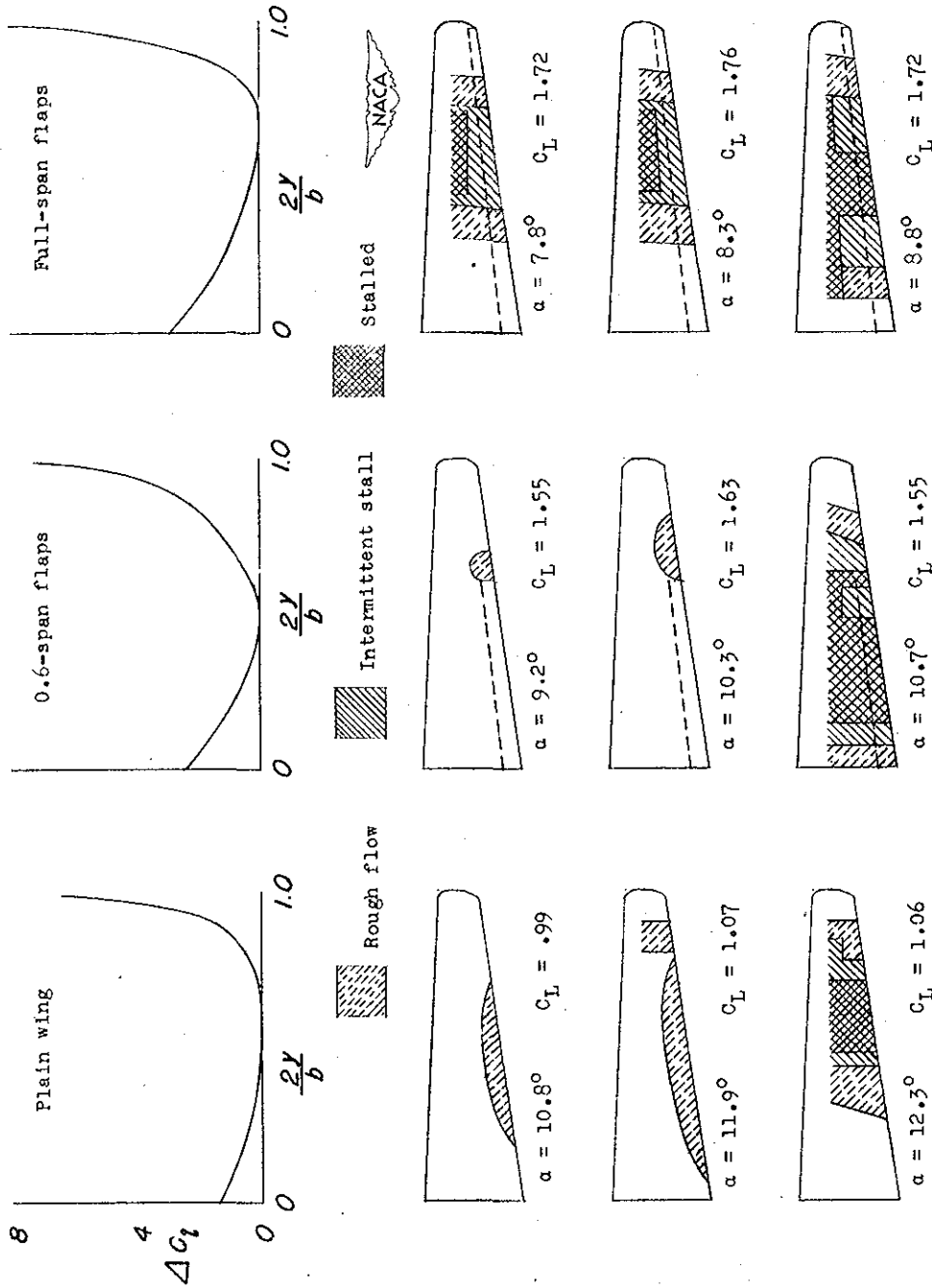
(d) NACA 65-210 sections; double slotted flaps.

Figure 13.- Concluded.



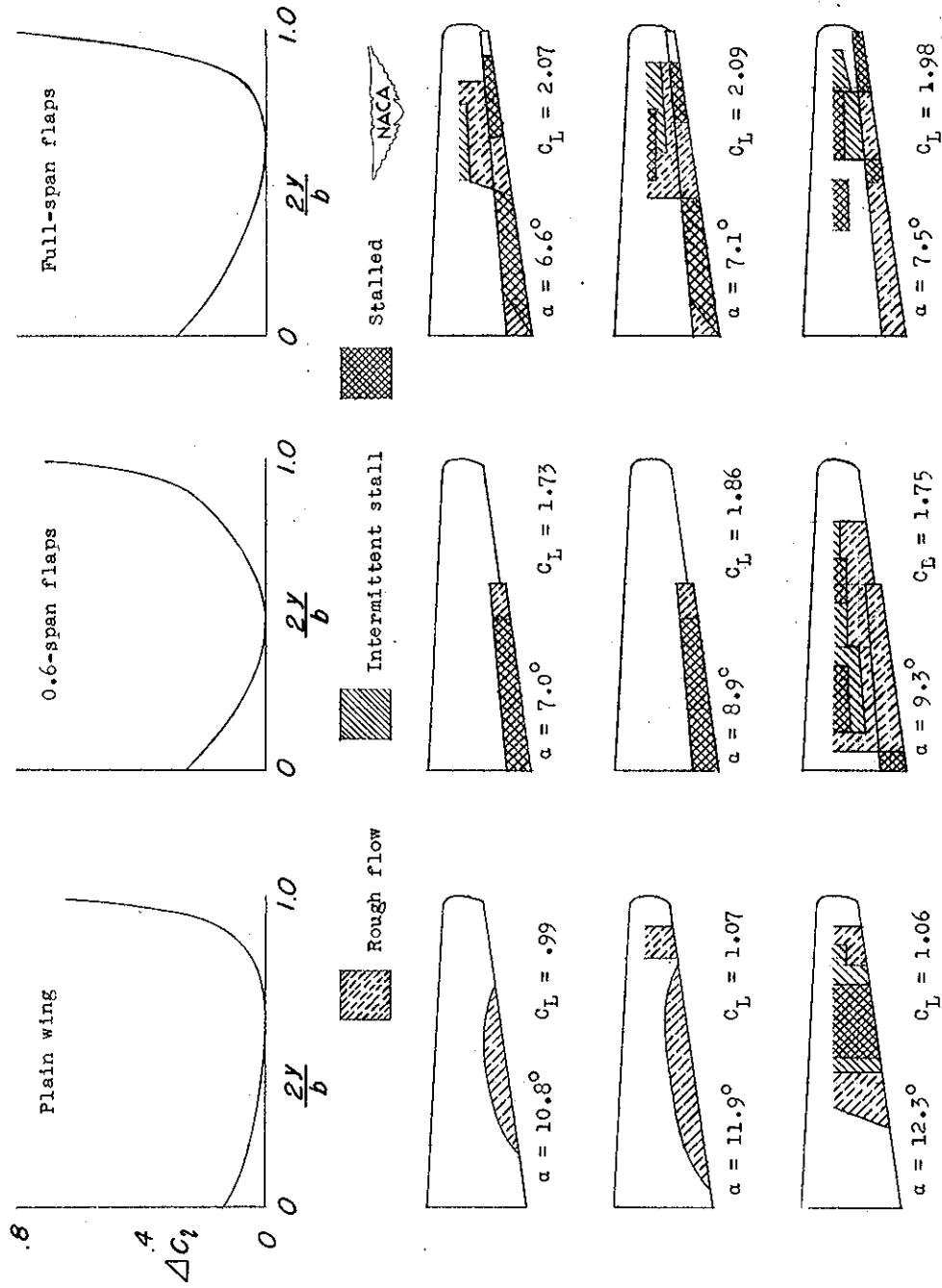
(a) NACA 64-210 sections; split flaps.

Figure 14.- Experimental and calculated stalling characteristics for wings with and without flaps; aspect ratio, 9.021; taper ratio, 0.4; washout, 2° .



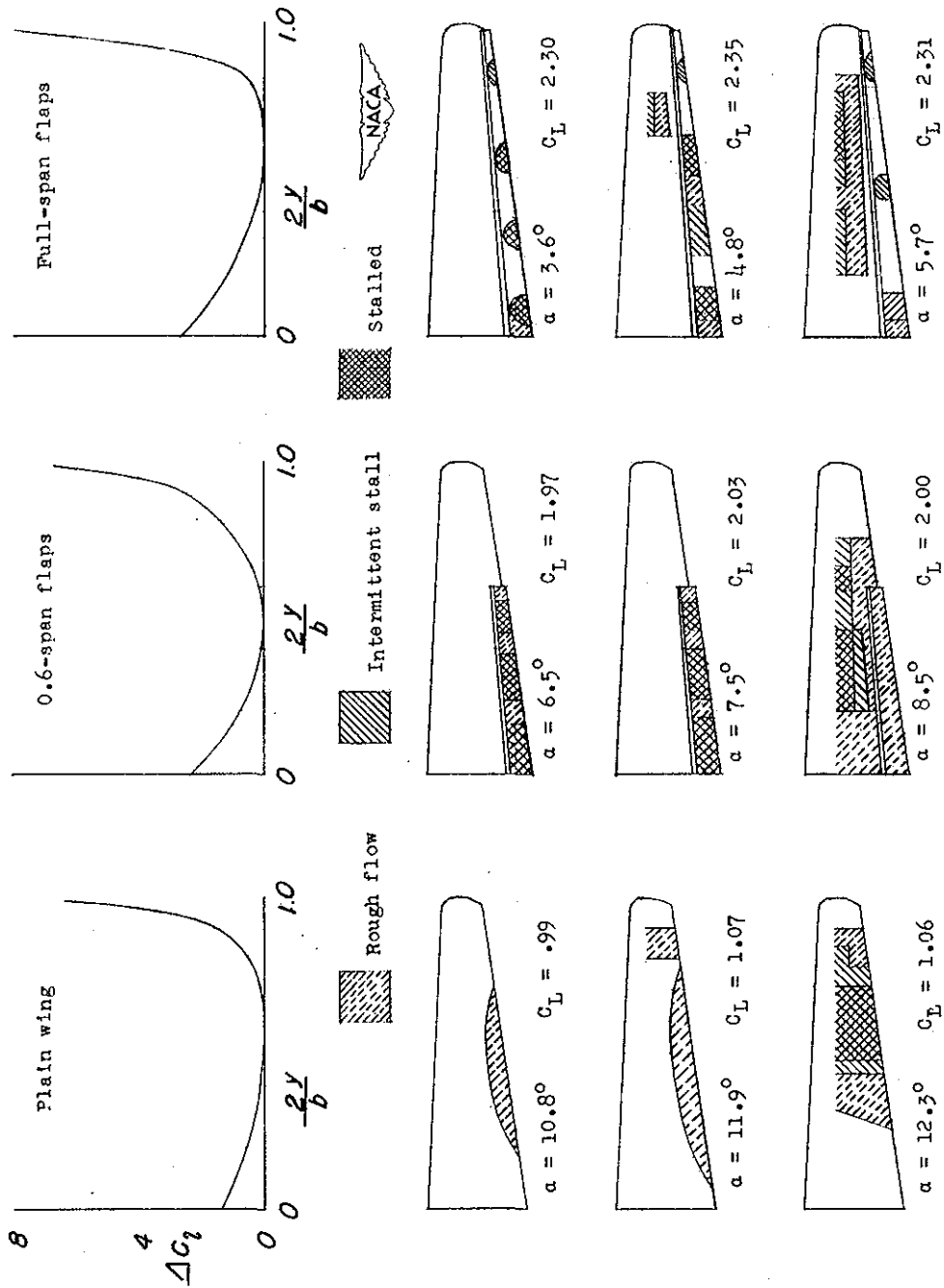
(b) NACA 65-210 sections; split flaps.

Figure 14.- Continued.



(c) NACA 65-210 sections; single slotted flaps.

Figure 14.- Continued.



(d) NACA 65-210 sections; double slotted flaps.

Figure 14.- Concluded.